tients with HIV infection: clinical manifestations, laboratory findings, and radiological features. J Infect Chemother 13: 1-7, 2007.
14. Del Palacio A, Llenas-Garcia J, Soledad Cuetara M, et al. Serum (1-->3) beta-D-Glucan as a noninvasive adjunct marker for the diagnosis and follow-up of Pneumocystis jiroveci pneumonia in patients with HIV infection. Clin Infect Dis 50: 451-452, 2010.
15. Shimizu A, Oka H, Matsuda T, Ozaki S. (1-->3)-beta-D glucan is a diagnostic and negative prognostic marker for Pneumocystis carinii pneumonia in patients with connective tissue disease. Clin Exp Rheumatol 23: 678-680, 2005.
16. Mori S, Cho I, Ichiyasu H, Sugimoto M. Asymptomatic carriage of Pneumocystis jiroveci in elderly patients with rheumatoid arthritis in Japan: a possible association between colonization and development of Pneumocystis jiroveci pneumonia during low-dose MTX therapy. Mod Rheumatol 18: 240-246, 2008.
17. Persat F, Ranque S, Derouin F, Michel-Nguyen A, Picot S, Sulahian A. Contribution of the (1-->3)-beta-D-glucan assay for diagnosis of invasive fungal infections. J Clin Microbiol 46: 1009-1013, 2008.
18. Obayashi T, Yoshida M, Mori T, et al. Plasma (1-->3)-beta-D-glucan measurement in diagnosis of invasive deep mycosis and fungal febrile episodes. Lancet 345: 17-20, 1995.
19. Ostrosky-Zeichner L, Alexander BD, Kett DH, et al. Multicenter clinical evaluation of the (1-->3) beta-D-glucan assay as an aid to diagnosis of fungal infections in humans. Clin Infect Dis 41: 654-659, 2005.
20. de Boer MG, Gelinck LB, van Zelst BD, et al. beta-d-Glucan and S-adenosylmethionine serum levels for the diagnosis of Pneumocystis pneumonia in HIV-negative patients: A prospective study. J Infect 62: 93-100, 2011.
21. Desmet S, Van Wijngaerden E, Maertens J, et al. Serum (1-3)-beta-D-glucan as a tool for diagnosis of Pneumocystis jirovecii pneumonia in patients with human immunodeficiency virus infection or hematological malignancy. J Clin Microbiol 47: 3871-3874, 2009.

Molecular Immunology 48 (2011) 2198–2202

Contents lists available at ScienceDirect

Molecular Immunology

journal homepage: www.elsevier.com/locate/molimm

Short communication

Plasticity of human CD8αα binding to peptide–HLA-A*2402

Yi Shi[a,b,c], Jianxun Qi[a,b], Aikichi Iwamoto[c,d], George F. Gao[a,b,c,e,*]

[a] CAS Key Laboratory of Pathogenic Microbiology and Immunology, Institute of Microbiology, Chinese Academy of Sciences, Beijing 100101, China
[b] Graduate University, Chinese Academy of Sciences, Beijing 100049, China
[c] China–Japan Joint Laboratory of Molecular Microbiology and Molecular Immunology, Institute of Microbiology, Chinese Academy of Sciences, Beijing 100101, China
[d] Division of Infectious Diseases, Advanced Clinical Research Center, Department of Infectious Diseases and Applied Immunology, Research Hospital, University of Tokyo, Minato-ku, 108-8639 Tokyo, Japan
[e] Research Network of Immunity and Health (rNIH), Beijing Institutes of Life Science, Chinese Academy of Sciences, Beijing 100101, China

ARTICLE INFO

Article history:
Received 7 April 2011
Received in revised form 6 May 2011
Accepted 9 May 2011
Available online 6 June 2011

Keywords:
Co-receptor
CD8
A24
Crystal structure
Molecular interaction
Plasticity
α3 domain loop shift

ABSTRACT

The human CD8 functions as a co-receptor for specific T cell recognition, and only one complex structure of human CD8αα binding to HLA-A*0201 has been solved, revealing the molecular basis of CD8 interacting with its ligand pHLA. Here, we present the complex structures of human CD8αα bound to HLA-A*2402, which demonstrate two opposite α3 domain CD loop shifts (either pull or push) in the HLA heavy chain upon CD8 engagement. Taking the previously reported mouse CD8–pMHC complex structures into account, from the structural view, all of the data indicate the plasticity of CD8 binding to pMHC/HLA, which facilitates its co-receptor function for T cells. The plasticity of CD8 binding appears not to affect the specificity of TCR recognition, as no peptide conformation change extends to the pMHC interface for TCR contacting.

1. Introduction

The T cell recognition of a peptide-major histocompatibility complex (pMHC) on the surface of an antigen presenting cell (APC) lies at the heart of the adaptive immune response, which is orchestrated by a number of protein–protein interactions (Rudolph et al., 2006), all contributing to the formation of the so-called immunological synapse (Grakoui et al., 1999). The specific identification of pMHC ligands is mediated by unique T cell receptors (TCRs) and by components of the multi-subunit CD3 complex, which transmit signals to the T cell. However, in the absence of co-receptor (CD8 or CD4) interaction, the immune recognition events, including cytokine production and cytotoxic effector function, are hampered (Laugel et al., 2007; Singer and Bosselut, 2004; Zamoyska, 1998). The CD8 or CD4 co-receptor can augment the TCR–pMHC interaction *in vivo*, and the effect of the co-receptor is qualitative during T cell activation but does not affect the specificity of the TCR–pMHC interaction (Gao et al., 2002). In addition, CD8 can bind to a non-classical MHC class I-like molecule, TL antigen, independent of a TCR and CD3, further expanding the function of CD8 as an immunomodulator (Cole and Gao, 2004; Gao and Jakobsen, 2000; Gao et al., 2002; Leishman et al., 2001; Wyer et al., 1999).

As a cell surface, disulfide-linked, dimeric glycoprotein, CD8 is expressed in a either CD8αα homodimer or CD8αβ heterodimer form, which has distinct cellular distributions and functions. Crystal structures of the human HLA-A*0201–CD8αα complex (Gao et al., 1997), murine MHC H-2Kb–CD8αα complex (Kern et al., 1998), murine H-2Dd–CD8αβ complex (Wang et al., 2009), TL antigen–CD8αα complex (Liu et al., 2003), and rhesus macaque CD8αα (Zong et al., 2009) have all been solved. In general, human CD8αα (hCD8αα), murine CD8αα (mCD8αα), and murine CD8αβ (mCD8αβ) bind to the protruding MHC α3 domain CD loop in an antibody-like manner. Previous kinetics data demonstrate that CD8αα and CD8αβ interact with MHC class I (MHCI) molecules in an allele-dependent but TCR- and peptide-independent manner (Gao et al., 2000; Huang et al., 2007). However, little is known about the molecular basis of CD8 binding to different MHCI alleles. Here, we solved the complex structure of hCD8αα bound to HLA-A*2402 to further elucidate the molecular basis of hCD8αα interacting with HLA alleles. Strikingly, comparing the two complex structures in

* Corresponding author at: CAS Key Laboratory of Pathogenic Microbiology and Immunology, Institute of Microbiology, Chinese Academy of Sciences, Beichen West Road, Beijing 100101, China. Tel.: +86 10 64807688, fax: +86 10 64807882.
E-mail address: gaof@im.ac.cn (G.F. Gao).

0161-5890/$ – see front matter © 2011 Elsevier Ltd. All rights reserved.
doi:10.1016/j.molimm.2011.05.009

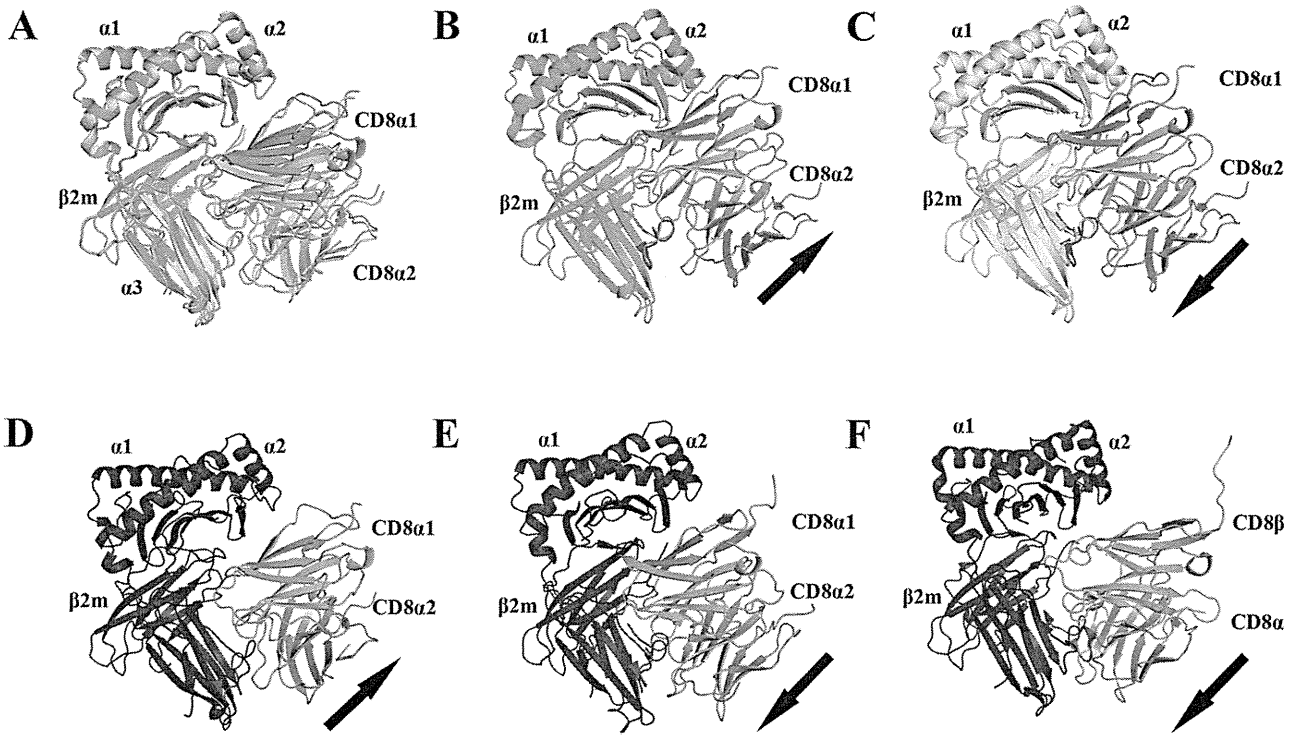

Fig. 1. Complex structures of all known human and murine CD8 molecules bound to pMHC ligands and superimposition of unliganded pMHCs indicates two conformations of α3 domain loop shifting (either pull or push) upon CD8 binding. To compare α3 domain loop shifts, partial structures in red represent the relative position of heavy chain amino acids 218–230 of the unliganded pMHC molecules. The proximal CD8 subunit is cyan, the distal CD8 subunit is pink, and liganded pMHC (A2, H-2K^b, or H-2D^d) is blue except for the hCD8αα/HLA-A24/peptide complexes solved in this study, which are colored differently (green for complex 1 and yellow for complex 2). (A) Superimposition of two hCD8αα/HLA-A24/peptide complexes in one crystallographic asymmetric unit solved in this study, in which the α1 and α2 domains of the heavy chain are superimposed very well for both complex 1 (green) and 2 (yellow). In hCD8αα/HLA-A24/peptide complex 1 (B) and hCD8αα/HLA-A2/peptide (D), the α3 domain loop is pulled toward the CD8. In hCD8αα/HLA-A24/peptide complex 2 (C), mCD8αα/H-2K^b/peptide (E), and mCD8αβ/H-2D^d/peptide (F), the α3 domain loop is pushed away from the CD8. Black arrows represent the directions of the α3 domain loop shift upon CD8 engagement. The PDB files used to prepare this figure are as follows: unliganded HLA-A2/peptide, 1HHJ; hCD8αα/HLA-A2/peptide, 1AKJ; unliganded H-2K^b/peptide, 2VAA; mCD8αα/H-2K^b/peptide, 1BHQ; unliganded H-2D^d/peptide, 3ECB; mCD8αβ/H-2D^d/peptide, 3DMM; unliganded HLA-A24/peptide, 3NFJ; and hCD8αα/HLA-A24/peptide, 3QZW.

the one asymmetric unit, opposite α3 domain CD loop shifts were observed upon hCD8αα binding to HLA-A*2402.

2. Materials and methods

2.1. Protein expression, refolding, and purification

Soluble hCD8αα protein and peptide–HLA-A*2402 complex (containing the HIV-1 Nef138-10 peptide, RYPLTFGWCF) were prepared as previously described (Cole et al., 2006, 2007; Gao et al., 1998). The individual proteins were then purified by Superdex^{TM} 200 10/300 GL gel-filtration chromatography (GE Healthcare).

2.2. Crystallization, data collection, and processing

All crystallization attempts were performed by the hanging drop vapor diffusion method at 18 °C with a protein/reservoir drop ratio of 1:1. For the HLA-A*2402/hCD8αα complex, a 1:1 molar ratio of A*2402/hCD8αα was mixed at a final concentration of 10 mg/ml for 6 h just before crystal trays were set up. Crystals were seen after 3–5 days in 0.1 M MES (pH 6.5) and 12% (w/v) polyethylene glycol 20,000. The crystals were briefly soaked in reservoir solution containing 17% (v/v) glycerol, mounted on the X-ray machine with a nylon loop, and then flash-cooled in a stream of gaseous nitrogen. Diffraction data were collected using beamline NE3A in the KEK synchrotron facility (Tsukuba, Japan) and ADSC Q270 imaging-plate detector at a wavelength of 1.0 Å. Data were indexed, integrated, and scaled using HKL2000 (Otwinowski and Minor, 1997). The data collection statistics are shown in Table 1.

Table 1
X-ray diffraction data processing and refinement statistics.

Data processing	
Space group	*P*1
Unit cell dimensions (*a*, *b*, *c*)	66.24, 67.02, 101.14
Unit cell dimensions (α, β, γ)	73.71, 71.84, 81.43
Resolution range (Å)	50.00–2.80 (2.90–2.80)[a]
Number of unique reflections	150,181
Molecules in the asymmetric unit	4
Redundancy	3.9 (3.6)[a]
Data completeness (%)	98.6 (95.6)[a]
R_{merge} (%)	6.1 (26.7)[a]
I/σ	22.5 (4.2)[a]
Refinement	
Resolution range (Å)	31.61–2.80
R_{cryst} (%)	20.5
R_{free} (%)	26.0
No. of atoms	
Protein	9922
Water	164
Average B-factor (Å^2)	
Protein	55.7
Water	46.0
RMS deviations from restraint target values	
Bond lengths (Å)	0.005
Bond angles (°)	0.823
Ramachandran plot statistics	
Most favored (%)	92.6
Allowed region (%)	7.4
Disallowed region (%)	0

[a] Values in parentheses are for the shell of highest resolution.

2.3. Structure determination, refinement, and analysis

Data were analyzed by molecular replacement using MolRep in CCP4 (CCP4, 1994). First, we searched the two HLA-A*2402–Nef138-10 molecules using the A24VYG molecule as the search model (Protein Data Bank (PDB) accession number, 2BCK). Then, we fixed the pHLA molecules and searched the two CD8αα molecules using the human CD8αα molecule (PDB accession number, 1AKJ) as the search model. All of the structures were further refined by several rounds of refinement using the PHENIX program (Adams et al., 2002), and the refinement statistics are described in Table 1.

The detailed interactions between HLA-A*2402 and hCD8αα were analyzed using Contact in the CCP4 package (CCP4, 1994). The PyMOL Molecular Graphics System (DeLano Scientific, http://www.pymol.org) was used to prepare figures.

2.4. Accession numbers

Atomic coordinates of the complex structures of HLA-A*2402/hCD8αα and free HLA-A*2402–Nef138-10 have been deposited in the PDB under accession numbers 3QZW and 3NFJ, respectively.

3. Results and discussion

3.1. Opposite α3 domain loop shifts

The crystals obtained in this study contain two hCD8αα/HLA-A*2402 complexes (complex 1 and complex 2) molecules per crystallographic asymmetric unit. The hCD8αα binds to the HLA-A*2402 MHCI molecule in a binding mode similar to that in the hCD8αα/HLA-A*0201 and mCD8αα/H-2K^b structures, involving contacts with the α2, α3, and β2m domains of the pMHC molecule. However, superimposition of the complex 1 and complex 2 structures (using the MHC α1 and α2 domains, residues 1–180, for the fit) revealed that different α3 domain movements are observed upon CD8αα binding (Fig. 1A). Further superimposition of an unliganded HLA-A*2402 structure with both of the complexes revealed that the α3 domain loops display opposite shifts in complexes 1 and 2 (Fig. 1B and C). In complex 1, the HLA-A*2402 α3 domain is "pulled" in toward the CD8 (Fig. 2A), but in complex 2, the HLA-A*2402 α3 domain is "pushed" away from CD8 (Fig. 2B). A similar "pulled-toward" conformation is seen in the hCD8αα/HLA-A*0201 complex,[11] (Gao et al., 1997) though with a larger movement (Fig. 1D), and a similar "pushed-away" conformation is evident in the mCD8αα/H-2K^b and mCD8αβ/H-2D^d structures (Fig. 1E and F), with different extents. However, we observed that two opposite α3 domain loop shifts can occur in the same HLA molecule bound to hCD8αα. These different conformations permit a degree of plasticity for hCD8αα binding to its ligand pMHC. A similar α3 domain movement is also seen in structures of the TCR–pMHC complex (Garboczi et al., 1996; Garcia et al., 1998). This plasticity appears to facilitate the formation of a stable tri-molecular complex (TCR/pMHC/CD8) for different TCRs binding to the pMHC. Such plasticity may also explain the previously reported slight differences in the binding affinities and kinetics of CD8 binding to different MHC/HLA alleles (Gao et al., 2000; Huang et al., 2007).

Although the hCD8αα binding to the HLA-A*2402 MHCI molecule shows a degree of plasticity, either in 'pulled-toward' conformation or in 'pushed-away' conformation, but no conformational change extends to the pHLA surface presented for TCR recognition (Fig. 3). This phenomenon is consistent with an avidity-based contribution from CD8 to TCR–pMHC interactions, and plasticity of CD8 binding appears not to affect the specificity of TCR recognition.

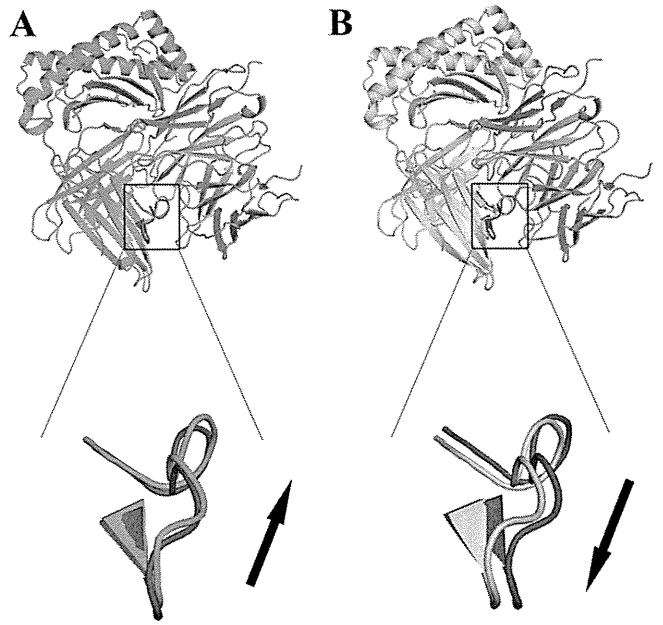

Fig. 2. Close-up view of the α3 domain loop shifting upon CD8 binding. (A) Complex 1 (green) shows a pulled-toward movement. (B) Complex 2 (yellow) shows a pushed-away movement. The detailed figure legend is referred to Fig. 1.

3.2. Tighter CD8αα binding in the pushed-away conformation

A detailed interaction analysis of hCD8αα binding to HLA-A*2402 was performed for both complexes (Table 2). The distance cutoff of the hydrogen bonds was ≤3.5 Å. In complex 1, 15 hydrogen bonds were formed between the CD8α1 subunit and HLA-A24 molecule, and four hydrogen bonds were formed between the CD8α2 subunit and the HLA-A24 heavy chain. In complex 2, the hydrogen bonds formed between the CD8α1 subunit and HLA-A*2402 molecule were equivalent to those in complex 1, but seven hydrogen bonds were formed between the CD8α2 subunit and the HLA-A*2402 heavy chain. Thus, more hydrogen bonds were formed in complex 2, indicating tighter CD8αα binding in the pushed-away conformation. We also compared the molecular interactions between hCD8αα/HLA-A*0201 and both of the hCD8αα/HLA-A*2402 complexes and found some allele-specific features (Table 2). Although hCD8αα binds to HLA-A*0201 in the same pulled-toward conformation as hCD8αα/HLA-A*2402 complex 1, more hydrogen bonds (20 hydrogen bonds) were formed between the CD8α1 subunit and the HLA-A*0201 molecule due to a larger α3 domain loop shift. However, the asymmetrical contributions of the two subunits of CD8αα are similar in hCD8αα/HLA-A*0201 and hCD8αα/HLA-A*2402 complex 1, with CD8α1 contributing approximately 75% of the total contacts. In the hCD8αα/HLA-A*2402 complex 1 with a pushed-away conformation, CD8α1 contributed approximately 60% of the total contacts, indicating that a greater contribution is derived from the CD8α2 subunit. Thus, the plasticity of hCD8αα binding to HLA-A*2402 is mediated by the contribution of the CD8α2 subunit.

Additional studies of the molecular architecture of co-receptor CD8 binding to different MHCI alleles is required to confirm the degrees of the plasticity of the CD8/pMHC (HLA) interaction. In conclusion, from the structural view, CD8 binding to pMHC displays some plasticity, which facilitates its co-receptor's function when interacting with T cells.

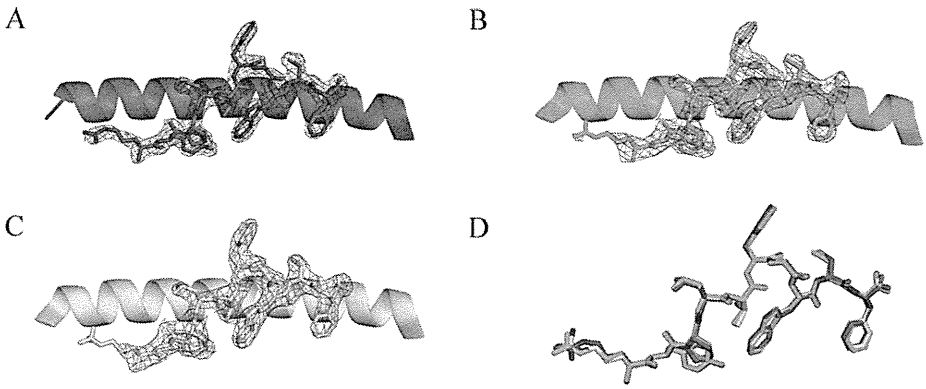

Fig. 3. Plasticity of hCD8αα binding to HLA-A24/peptide appears not to affect the peptide conformation. Electron density maps are shown unambiguously for peptide in unliganded pMHC (A), liganded pMHC of complex 1 (B), and liganded pMHC of complex 2 (C). (D) Superposition of those three peptides displays no conformation change.

Table 2
Interaction between CD8αα and HLA-A*2402 (A24)/HLA-A*0201 (A2).

CD8αα	MHC[a]	Length (Å) – complex 1–A24	Length (Å) – complex 2–A24	Length (Å) – A2
Hydrogen bonds (distance ≤ 3.5 Å)				
CD8α1				
R4 NE	D122 OD1	3.36	–	–
R4 NE	D122 OD2	2.55	3.27	2.96
R4 NH1	Q115 OE1	–	–	3.18
R4 NH2	Q155 OE1	3.47	–	–
R4 NH2	D122 OD1	3.20	2.53	3.04
R4 NH2	D122 OD2	–	2.87	–
K21 NZ	E128 OE1	–	–	2.91
K21 NZ	E128 OE2	–	–	2.75
S27 OG	E232 OE1	3.36	3.50	2.66
N28 OD1	V231 O	3.36	–	3.26
N28 OD1	E232 N	3.16	–	–
N28 OD1	E232 OE1	–	–	3.01
N28 OD1	K243 NZ	–	–	3.24
N28 ND2	L230 O	–	3.25	–
N28 ND2	E232 OE1	–	–	3.35
T30 OG1	T225 O	2.57	–	2.71
Q54 OE1	Q262 OE1	2.78	3.08	3.10
Q54 OE1	Q262 NE2	–	3.24	2.89
Q54 NE2	T214 OG1	–	2.61	3.36
N99 ND2	L230 O	3.36	–	3.38
N99 OD1	L230 N	2.59	2.95	3.00
N99 OD1	L230 O	3.23	3.28	–
S100 O	Q226 OE1	3.12	3.08	–
S100 O	Q226 NE2	–	–	3.01
S100 OG	Q226 O	2.77	2.71	2.73
D75 OD2	K58(β) NZ	3.00	3.28	2.68
V24 O	K58(β) NZ	–	3.49	2.98
R4 NH2	W60(β) NE1	–	3.43	–
Total		15	15	20
CD8α2				
S34 OG	Q226 OE1	3.29	2.68	–
S34 OG	Q226 NE2	–	3.34	3.05
Y51 OH	D227 OD1	3.03	3.04	3.47
Y51 OH	D227 OD2	3.33	3.17	3.01
N55 OD1	E198 OE2	–	3.36	–
N55 OD1	V248 O	–	–	3.23
N99 OD1	E222 OE1	3.14	2.76	–
N99 N	E222 OE1	–	3.44	–
Total		4	7	4

CD8αα	MHC	Complex 1 (A24)	Complex 2 (A24)	A2
Contacts between HLA-A24/HLA-A24 and CD8αα (distance ≤ 4 Å)				
CD8α1	Heavy chain	82 (64.57%)	67 (51.94%)	99 (69.23%)
CD8α1	β2m	15 (11.81%)	11 (8.53%)	11 (7.69%)
CD8α2	Heavy chain	29 (22.83%)	50 (38.76%)	33 (23.08%)
CD8α2	β2m	1 (0.79%)	1 (0.78%)	0
Total		127	129	143

[a] Residues for the MHC are from the heavy chain unless marked (β).

Acknowledgements

This work was supported by National Natural Science Foundation of China (NSFC, grant No. 31030030), and GFG is a leading principal investigator of the NSFC Innovative Research Group (grant No. 81021003).

References

Adams, P.D., Grosse-Kunstleve, R.W., Hung, L.W., Ioerger, T.R., McCoy, A.J., Moriarty, N.W., Read, R.J., Sacchettini, J.C., Sauter, N.K., Terwilliger, T.C., 2002. PHENIX: building new software for automated crystallographic structure determination. Acta Crystallogr. D: Biol. Crystallogr. 58, 1948–1954.

CCP4, 1994. The CCP4 suite: programs for protein crystallography. Acta Crystallogr. D: Biol. Crystallogr. 50, 760–763.

Cole, D.K., Gao, G.F., 2004. CD8: adhesion molecule, co-receptor and immunomodulator. Cell. Mol. Immunol. 1, 81–88.

Cole, D.K., Rizkallah, P.J., Gao, F., Watson, N.I., Boulter, J.M., Bell, J.I., Sami, M., Gao, G.F., Jakobsen, B.K., 2006. Crystal structure of HLA-A*2402 complexed with a telomerase peptide. Eur. J. Immunol. 36, 170–179.

Cole, D.K., Rizkallah, P.J., Boulter, J.M., Sami, M., Vuidepot, A.L., Glick, M., Gao, F., Bell, J.I., Jakobsen, B.K., Gao, G.F., 2007. Computational design and crystal structure of an enhanced affinity mutant human CD8αα coreceptor. Proteins 67, 65–74.

Gao, G.F., Gerth, U.C., Wyer, J.R., Willcox, B.E., O'Callaghan, C.A., Zhang, Z., Jones, E.Y., Bell, J.I., Jakobsen, B.K., 1998. Assembly and crystallization of the complex between the human T cell coreceptor CD8α homodimer and HLA-A2. Protein Sci. 7, 1245–1249.

Gao, G.F., Jakobsen, B.K., 2000. Molecular interactions of coreceptor CD8 and MHC class I: the molecular basis for functional coordination with the T-cell receptor. Immunol. Today 21, 630–636.

Gao, G.F., Tormo, J., Gerth, U.C., Wyer, J.R., McMichael, A.J., Stuart, D.I., Bell, J.I., Jones, E.Y., Jakobsen, B.K., 1997. Crystal structure of the complex between human CD8α(α) and HLA-A2. Nature 387, 630–634.

Gao, G.F., Willcox, B.E., Wyer, J.R., Boulter, J.M., O'Callaghan, C.A., Maenaka, K., Stuart, D.I., Jones, E.Y., Van Der Merwe, P.A., Bell, J.I., Jakobsen, B.K., 2000. Classical and nonclassical class I major histocompatibility complex molecules exhibit subtle conformational differences that affect binding to CD8αα. J. Biol. Chem. 275, 15232–15238.

Gao, G.F., Rao, Z., Bell, J.I., 2002. Molecular coordination of αβ T-cell receptors and coreceptors CD8 and CD4 in their recognition of peptide-MHC ligands. Trends Immunol. 23, 408–413.

Garboczi, D.N., Ghosh, P., Utz, U., Fan, Q.R., Biddison, W.E., Wiley, D.C., 1996. Structure of the complex between human T-cell receptor, viral peptide and HLA-A2. Nature 384, 134–141.

Garcia, K.C., Degano, M., Pease, L.R., Huang, M., Peterson, P.A., Teyton, L., Wilson, I.A., 1998. Structural basis of plasticity in T cell receptor recognition of a self peptide-MHC antigen. Science 279, 1166–1172.

Grakoui, A., Bromley, S.K., Sumen, C., Davis, M.M., Shaw, A.S., Allen, P.M., Dustin, M.L., 1999. The immunological synapse: a molecular machine controlling T cell activation. Science 285, 221–227.

Huang, J., Edwards, L.J., Evavold, B.D., Zhu, C., 2007. Kinetics of MHC–CD8 interaction at the T cell membrane. J. Immunol. 179, 7653–7662.

Kern, P.S., Teng, M.K., Smolyar, A., Liu, J.H., Liu, J., Hussey, R.E., Spoerl, R., Chang, H.C., Reinherz, E.L., Wang, J.H., 1998. Structural basis of CD8 coreceptor function revealed by crystallographic analysis of a murine CD8αα ectodomain fragment in complex with H-2Kb. Immunity 9, 519–530.

Laugel, B., van den Berg, H.A., Gostick, E., Cole, D.K., Wooldridge, L., Boulter, J., Milicic, A., Price, D.A., Sewell, A.K., 2007. Different T cell receptor affinity thresholds and CD8 coreceptor dependence govern cytotoxic T lymphocyte activation and tetramer binding properties. J. Biol. Chem. 282, 23799–23810.

Leishman, A.J., Naidenko, O.V., Attinger, A., Koning, F., Lena, C.J., Xiong, Y., Chang, H.C., Reinherz, E., Kronenberg, M., Cheroutre, H., 2001. T cell responses modulated through interaction between CD8αα and the nonclassical MHC class I molecule, TL. Science 294, 1936–1939.

Liu, Y., Xiong, Y., Naidenko, O.V., Liu, J.H., Zhang, R., Joachimiak, A., Kronenberg, M., Cheroutre, H., Reinherz, E.L., Wang, J.H., 2003. The crystal structure of a TL/CD8αα complex at 2.1 A resolution: implications for modulation of T cell activation and memory. Immunity 18, 205–215.

Otwinowski, Z., Minor, W., 1997. Processing of X-ray diffraction data collected in oscillation mode. Methods Enzymol. 276, 307–326.

Rudolph, M.G., Stanfield, R.L., Wilson, I.A., 2006. How TCRs bind MHCs, peptides, and coreceptors. Annu. Rev. Immunol. 24, 419–466.

Singer, A., Bosselut, R., 2004. CD4/CD8 coreceptors in thymocyte development, selection, and lineage commitment: analysis of the CD4/CD8 lineage decision. Adv. Immunol. 83, 91–131.

Wang, R., Natarajan, K., Margulies, D.H., 2009. Structural basis of the CD8αβ/MHC class I interaction: focused recognition orients CD8β to a T cell proximal position. J. Immunol. 183, 2554–2564.

Wyer, J.R., Willcox, B.E., Gao, G.F., Gerth, U.C., Davis, S.J., Bell, J.I., van der Merwe, P.A., Jakobsen, B.K., 1999. T cell receptor and coreceptor CD8αα bind peptide-MHC independently and with distinct kinetics. Immunity 10, 219–225.

Zamoyska, R., 1998. CD4 and CD8: modulators of T-cell receptor recognition of antigen and of immune responses? Curr. Opin. Immunol. 10, 82–87.

Zong, L., Chen, Y., Peng, H., Gao, F., Iwamoto, A., Gao, G.F., 2009. Rhesus macaque: a tight homodimeric CD8αα. Proteins 75, 241–244.

Journal of Medicinal Chemistry

ARTICLE

pubs.acs.org/jmc

Design of HIV-1 Protease Inhibitors with C3-Substituted Hexahydrocyclopentafuranyl Urethanes as P2-Ligands: Synthesis, Biological Evaluation, and Protein−Ligand X-ray Crystal Structure†

Arun K. Ghosh,*[,‡] Bruno D. Chapsal,[‡] Garth L. Parham,[‡] Melinda Steffey,[‡] Johnson Agniswamy,[§] Yuan-Fang Wang,[§] Masayuki Amano,[∥] Irene T. Weber,[§] and Hiroaki Mitsuya[∥,⊥]

[‡]Departments of Chemistry and Medicinal Chemistry, Purdue University, West Lafayette, Indiana 47907, United States

[§]Department of Biology, Molecular Basis of Disease, Georgia State University, Atlanta, Georgia 30303, United States

[∥]Departments of Hematology and Infectious Diseases, Kumamoto University Graduate School of Medical and Pharmaceutical Sciences, Kumamoto 860-8556, Japan

[⊥]Experimental Retrovirology Section, HIV and AIDS Malignancy Branch, National Cancer Institute, National Institutes of Health, Bethesda, Maryland 20892, United States

Supporting Information

ABSTRACT: We report the design, synthesis, biological evaluation, and the X-ray crystal structure of a novel inhibitor bound to the HIV-1 protease. Various C3-functionalized cyclopentanyltetrahydrofurans (Cp-THF) were designed to interact with the flap Gly48 carbonyl or amide NH in the S2-subsite of the HIV-1 protease. We investigated the potential of those functionalized ligands in combination with hydroxyethylsulfonamide isosteres. Inhibitor **26** containing a 3-(*R*)-hydroxyl group on the Cp-THF core displayed the most potent enzyme inhibitory and antiviral activity. Our studies revealed a preference for the 3-(*R*)-configuration over the corresponding 3-(*S*)-derivative. Inhibitor **26** exhibited potent activity against a panel of multidrug-resistant HIV-1 variants. A high resolution X-ray structure of **26**-bound HIV-1 protease revealed important molecular insight into the ligand-binding site interactions.

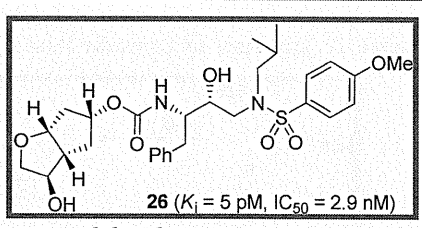

INTRODUCTION

Human immunodeficiency virus 1 (HIV-1) protease inhibitors are critical components of antiretroviral therapies.[1,2] However, the emergence of drug resistance has raised serious questions about long-term treatment options.[3,4] Our structure-based design of inhibitors targeting the protein backbone has led to the discovery of a variety of novel HIV-1 protease inhibitors (PIs) with broad-spectrum activity against multidrug-resistant HIV-1 variants.[5,6] One of these inhibitors, darunavir (**1**, Figure 1), was approved by the FDA for the treatment of HIV/AIDS patients.[7−9] In an effort to address drug resistance, our inhibitor design strategy focused on maximizing active site interactions with the protease, particularly by promoting extensive hydrogen bonding interactions with backbone atoms throughout the active site.[5,6]

We have recently reported a number of potent inhibitors incorporating a stereochemically defined (3a*S*,5*R*,6a*R*)-hexahydro-2*H*-cyclopenta[*b*]furan-5-yl (Cp-THF) as the P2-ligand with a modified hydroxyethylsulfonamide isostere as in inhibitor **3**.[10] The X-ray crystal structure of **3**-bound HIV-1 protease revealed the formation of an extensive hydrogen-bonding network between the inhibitor and the active site. On the basis of this molecular insight, we subsequently incorporated a stereochemically defined lactam at the P1′-position to further enhance backbone interactions.[11] Interestingly, the resulting inhibitor **4** retained full potency against a range of multidrug-resistant HIV-1 variants.[12] The X-ray structural studies of **4**-bound HIV-1 protease evidenced enhanced backbone interactions with the Gly27′ carbonyl at the S1′-subsite. The Cp-THF ligand appears to fit within the S2-subsite, and the cyclic ether oxygen is involved in a close hydrogen bonding interaction with the backbone NH of Asp29 (2.8 Å). On the basis of this molecular insight, we have now investigated structural modifications of the Cp-THF ligand to further optimize ligand binding, particularly hydrogen bonding ability, in the S2-subsite. The X-ray structure of **3**-bound HIV-1 protease indicated that the C3 methylene of the Cp-THF is in proximity to the protease flap region. In fact, the X-ray data suggested a weak C3−H···O interaction with the Gly48 backbone carbonyl group.[10] We therefore envisioned that introduction of a polar substituent at the C3 position may lead to additional interactions of the Cp-THF ligand with the protease flap residues. Furthermore, an inhibitor that makes tight interactions with the protease flap region could conceivably delay its dissociation via opening of the flaps. Herein, we report the design, synthesis, and biological evaluation of a series of protease inhibitors that incorporate a stereochemically defined functionality at the C3 position of the Cp-THF ligand. Inhibitor **26**,

Received: May 20, 2011
Published: July 29, 2011

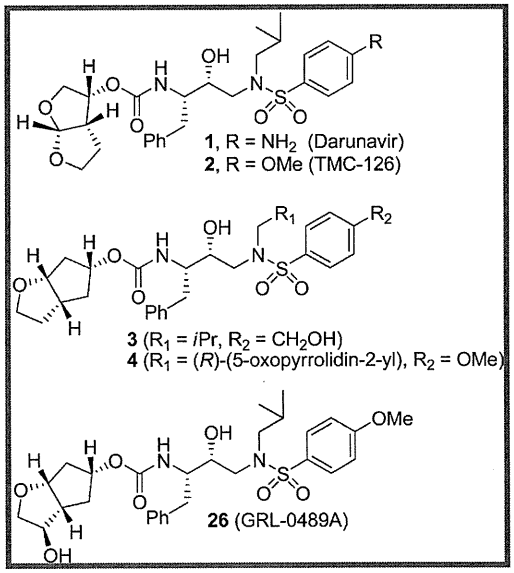

Figure 1. Structures of potent HIV-1 protease inhibitors **1**−**4** and **26**.

Scheme 1. Syntheses of Optically Pure P2 Ligands 7 and 8

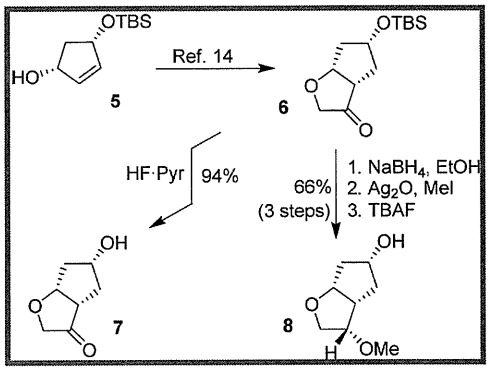

incorporating a 3-(*R*)-hydroxyl group, was the most potent PI (K_i = 5 pM; antiviral IC_{50} = 2.9 nM). This inhibitor also maintained excellent potency against a range of multidrug-resistant HIV-1 variants. The protein−ligand X-ray structure of **26**-bound HIV-1 protease revealed important insights into the ligand-binding site interactions of the inhibitor with the flap region as well as other regions of the HIV-1 protease active site.

CHEMISTRY

The syntheses of 3-keto and 3-(*S*)-methoxy Cp-THF ligands are shown in Scheme 1. Optically active alcohol **5** was prepared in multigram quantities as described previously.[13,14] This was efficiently converted to ketone **6** as reported by us.[14] The removal of TBS ether by exposure to HF−pyridine afforded keto alcohol **7** in 94% yield. Ketone **6** was converted to 3-(*S*)-methoxy derivative **8** in a three-step sequence involving (1) reduction of the ketone with $NaBH_4$ in ethanol at −25 °C to provide the corresponding alcohol as a single diastereomer, (2) methylation of the resulting alcohol with MeI in the presence of Ag_2O in acetonitrile, and (3) removal of the silyl group with TBAF in THF to provide **8** in 66% yield, in three steps.

The syntheses of 3-(*R*)-acetoxy and 3-(*R*)-methoxy ligands **11** and **12** are outlined in Scheme 2. Treatment of alcohol **5** with

Scheme 2. Syntheses of Ligands 11 and 12

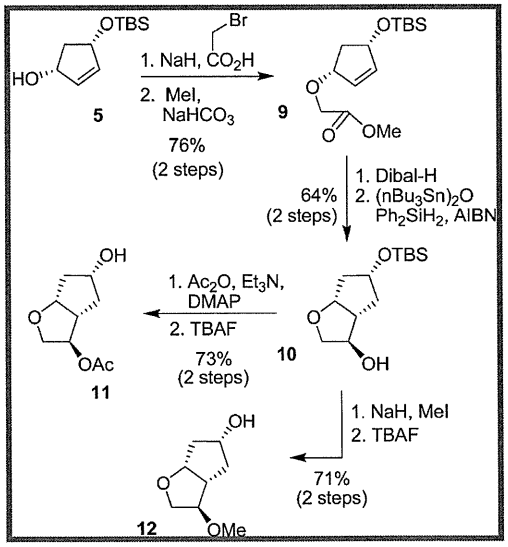

Scheme 3. Syntheses of C3-Methyl-Substituted Ligands 14 and 18

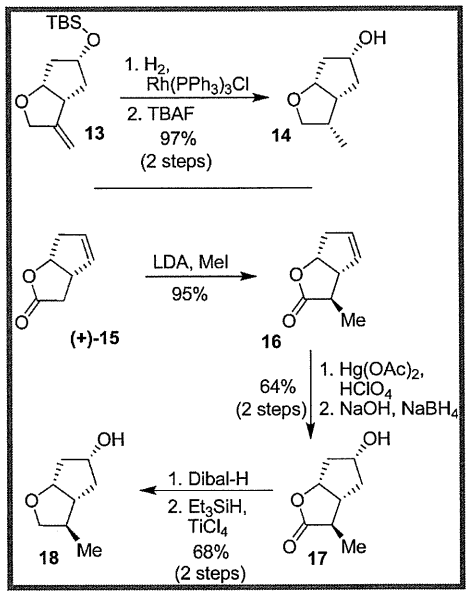

NaH and 2-bromoacetic acid in THF provided the corresponding alkylated acid. The resulting acid was reacted with methyl iodide in the presence of $NaHCO_3$ to provide methyl ester **9** in 76% yield (two steps). DIBAL-H reduction of ester **9** followed by radical cyclization[15] of the resulting alkene using a catalytic amount of $(n\text{-}Bu_3Sn)_2O$, Ph_2SiH_2 and ethanol (2 equiv) in the presence of a catalytic amount of AIBN in benzene provided 3-(*R*)-hydroxy derivative **10** in 64% yield, in two steps. The ^1H NMR results showed a diastereomeric ratio of 10:1. The major isomer was separated by silica gel chromatography and used for the subsequent reactions. Reaction of alcohol **10** with acetic anhydride and triethylamine in the presence of a catalytic amount of DMAP afforded the corresponding acetate. The removal of the silyl group with TBAF in THF provided ligand **11** in 73% yield, in two steps. Alcohol **10** was converted to methoxy derivative **12** by

Scheme 4. Syntheses of Activated Mixed Carbonates 19a–f

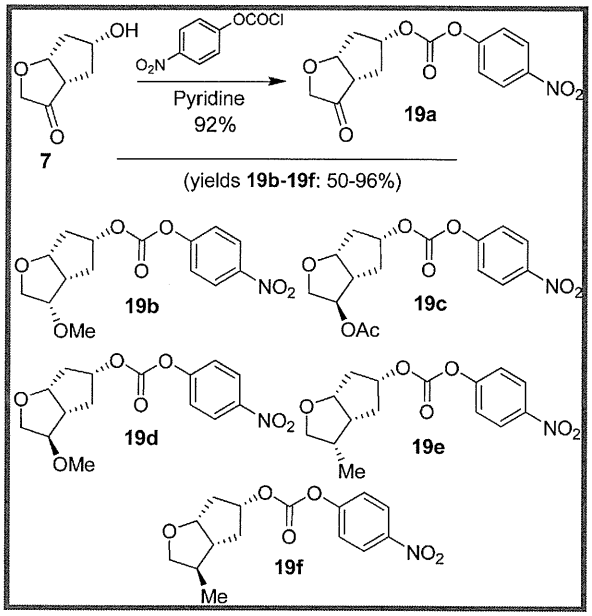

alkylation with NaH and MeI in THF followed by removal of the silyl group in 71% yield (two steps).

We also planned to synthesize stereochemically defined 3-methyl derivatives to compare with the effects of alkoxy and hydroxy groups. Toward this goal, we have carried out stereoselective syntheses of 3-(*S*)- and 3-(*R*)-methyl derivatives, and the synthetic routes are shown in Scheme 3. Optically active olefin **13** was synthesized as described previously.[14] Catalytic hydrogenation of **13** in the presence of Wilkinson's catalyst under a hydrogen filled balloon at 23 °C for 3 h followed by removal of the silyl group using TBAF afforded 3-(*S*)-methyl derivative **14**.[16] For the synthesis of the 3-(*R*)-methyl derivative, commercially available optically active lactone (+)-**15** was methylated using LDA and MeI at −78 °C to provide methyl derivative **16** with high diastereoselectivity (dr = 20:1) and in 95% yield. Olefin **16** was then subjected to oxymercuration condition with $Hg(OAc)_2$ and $HClO_4$. The resulting organomercurial derivative was treated with aqueous sodium hydroxide solution followed by $NaBH_4$ reduction to afford *endo*-alcohol **17** in 64% yield. The lactone was then reduced to the corresponding lactol with DIBAL-H. Further reduction of the resulting lactol using Et_3SiH and $TiCl_4$ furnished 3-(*R*)-methyl derivative **18** in 68% yield. Results from the ^1H NMR NOESY experiments fully corroborated the assignment of 3-(*S*)- and 3-(*R*)-stereochemistry of methyl derivatives **14** and **18**, respectively.

Various optically active ligand alcohols **7**, **8**, **11**, **12**, **14**, and **18** were converted to the respective mixed activated carbonates. As shown in Scheme 4, reactions of ligand alcohols with 4-nitrophenyl chloroformate in the presence of pyridine in CH_2Cl_2 provided activated carbonates **19a–f** in 50–96% yield.[17] The syntheses of designed inhibitors were carried out by coupling these activated carbonates with various hydroxyethylsulfonamide isosteres containing functionalized P2′-phenylsulfonamide ligands. As shown in Scheme 5, amines **20a–c** were readily prepared as described previously.[10,17] Reaction of amine **20a** with carbonate **19a** provided inhibitor **21**. Inhibitors **22–24** were prepared by reaction of carbonate **19a** with respective amines **20a–c** followed by $NaBH_4$ reduction of the resulting ketone derivatives.

Scheme 5. Syntheses of Inhibitors 21–32

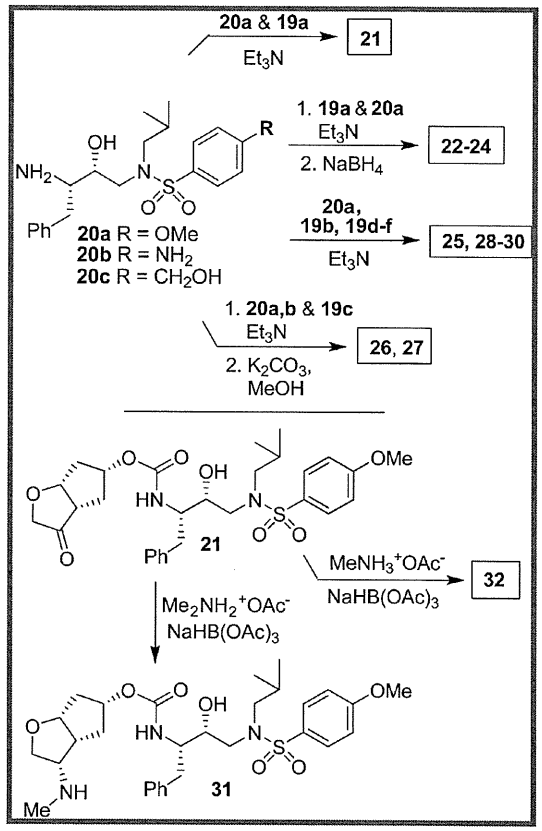

The inhibitor structures are shown in Table 1. Inhibitors **25** and **28–30** were prepared by reactions of amine **20a** with mixed carbonates **19b** and **19d–f**, respectively. The synthesis of inhibitors **26** and **27** was carried out by reactions of mixed carbonate **19c** with amines **20a** and **20b** followed by removal of the acetyl group with K_2CO_3 in methanol. All inhibitors were prepared in good to excellent overall (41–96%) yields. The synthesis of inhibitor **31** containing a dimethylamine functionality was carried out by reductive amination of ketone **21** with $Me_2NH_2{}^+OAc^-$ in the presence of $NaHB(OAc)_3$. We have also attempted to prepare the corresponding methylamine derivative by reductive amination with $MeNH_3{}^+OAc^-$. However, the resulting 3-(*S*)-methylamine derivative **32** turned out to be unstable.

RESULTS AND DISCUSSION

As mentioned previously, inhibitors were designed to make additional interactions in the S2-subsite of the protease, especially with the Gly48 backbone atoms in the flap region of the enzyme. All inhibitors in Table 1 were first evaluated in enzyme inhibitory assay developed by Toth and Marshall.[18] Inhibitors that exhibited potent K_i were subsequently evaluated for in vitro antiviral assays. As can be seen in the Table 1, all inhibitors displayed subnanomolar to low picomolar inhibitory potencies. Inhibitor **22**, with a 3-(*S*)-hydroxy group on the Cp-THF, was significantly more potent than the keto derivative **21** (entries 1 and 2). The 3-(*S*)-hydroxy Cp-THF ligand was also investigated in combination with other phenylsulfonamide substituents. Inhibitor **23** with a *p*-aminophenylsulfonamide as the P2′-ligand displayed impressive inhibitory potency; however, its antiviral

dx.doi.org/10.1021/jm200649p | *J. Med. Chem.* 2011, 54, 5890–5901

Table 1. Enzymatic Inhibitory and Antiviral Activity of Inhibitors 21−31

Entry	Inhibitor	K_i (nM)	IC_{50} (nM)[a]	Entry	Inhibitor	K_i (nM)	IC_{50} (nM)[a]
1	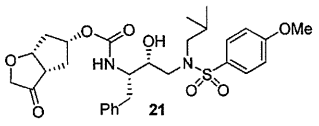 **21**	0.95	14	7	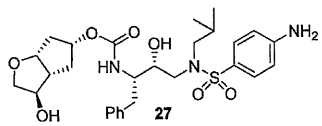 **27**	0.006	36
2	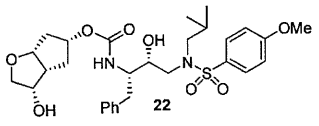 **22**	0.077	7	8	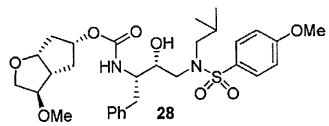 **28**	0.006	3.4
3	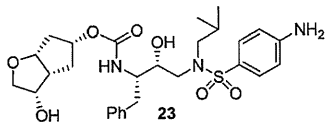 **23**	0.079	25	9	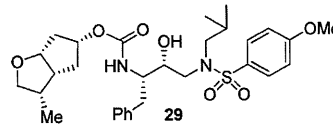 **29**	0.16	25
4	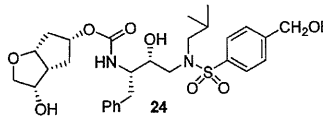 **24**	0.06	19	10	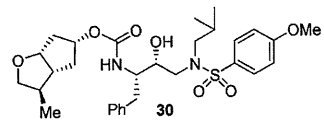 **30**	0.017	---
5	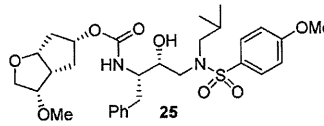 **25**	0.39	37	11	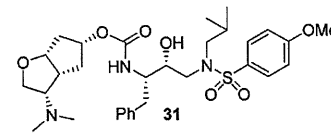 **31**	12.5	---
6	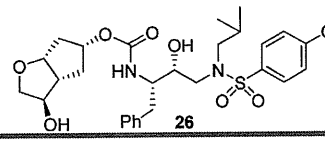 **26**	0.005	2.9				

[a] Values are the mean of at least two experiments. Human T-lymphoid (MT-2) cells (2×10^3) were exposed to 100 $TCID_{50}$ of HIV-1_{LAI} and cultured in the presence of each PI, and IC_{50} values were determined using the MTT assay. The IC_{50} values of amprenavir (APV), saquinavir (SQV), indinavir (IDV), and darunavir (DRV) were 0.03, 0.015, 0.03, and 0.003 μM, respectively.

activity was 3-fold lower than **22**. Inhibitor **24** with a *p*-hydroxymethylphenylsulfonamide as the P2′-ligand has shown a reduction in potency. Inhibitor **25**, which contains a 3-(*S*)-methoxy substituent, exhibited a significant loss of potency and a near 5-fold loss of antiviral activity compared to **22**. Interestingly, inhibitor **26** with 3-(*R*) configuration displayed an impressive enzyme inhibitory and antiviral activity. Inhibitor **27** with the 4-aminophenylsulfonamide isostere also showed comparable enzyme inhibitory activity. Inhibitor **28**, with a 3-(*R*)-methoxy group, also exhibited comparable inhibitory potency.

In order to probe the importance of the C3- oxygen on the Cp-THF ring, inhibitors **29** and **30** with a methyl group in place of a C3-hydroxyl were synthesized. Inhibitor **29**, which contains a 3-(*S*)-methyl group, showed a significant reduction in potency compared to **22**. Similarly, inhibitor **30** with a 3-(*R*)-methyl group has shown a reduction in enzyme K_i compared to the corresponding hydroxy derivative **26**. We have also investigated an amine substitution on the Cp-THF ligand. Inhibitor **31** with C3-dimethylamine exhibited a substantially lower enzyme inhibitory potency compared to the corresponding hydroxy or methoxy derivatives.

Inhibitors **22** with a 3-(*S*)-hydroxyl group and **26** with a 3-(*R*)-hydroxyl group on the Cp-THF ligand were tested against a panel of multidrug-resistant HIV-1 variants. Their antiviral activity was compared against other clinically available PIs including APV and DRV. The results are shown in Table 2. All inhibitors in Table 2 exhibited high antiviral activity against the wild-type HIV-1 laboratory strain, HIV-$1_{ERS104pre}$, isolated from a drug-naive patient.[7] Compound **26** provided the most potent activity with an IC_{50} of 2.9 nM, comparable to that of DRV. When tested against various multidrug-resistant HIV-1 strains, the IC_{50} of inhibitor **26** remained in the low nanomolar range (2.9−29 nM) and fold-change in IC_{50} did not exceed 10. Interestingly, isomeric inhibitor **22** displayed lower activity against the wild-type viral strain (IC_{50} = 20 nM). It also exhibited a much larger IC_{50} fold change and in some cases only marginal activity against multidrug-resistant HIV-1 variants. Such a stark contrast in antiviral activity of **22** compared to **26** emphasizes the importance of the stereochemistry at the C3-position of the Cp-THF ligand. Inhibitor **26** displayed a superior profile compared to another approved PI, APV. Overall, inhibitor **26** maintained impressive potency against all tested multidrug-resistant HIV-1 strains. It compared favorably with DRV, which is the leading PI for the treatment of multidrug resistant HIV infection.

In order to gain molecular insight into the ligand/binding-site interactions responsible for the activity of inhibitor **26**, we have determined the X-ray crystal structure of the inhibitor-bound wild-type HIV-1 protease that was refined to a 1.45 Å resolution. The protease dimer binds with the inhibitor in two orientations

Table 2. Comparison of the Antiviral Activity of 22, 26, and Other PIs against Multidrug Resistant HIV-1 Variants

	$IC_{50} \pm SD$, μM (fold change)[b]			
virus[a]	APV	DRV	22	26
HIV-$1_{ERS104pre}$(wt)	0.030 ± 0.006	0.0037 ± 0.0001	0.020 ± 0.004	0.0029 ± 0.0008
HIV-$1_{MDR/B}$	0.93 ± 0.28 (31)	0.036 ± 0.013 (10)	>1 (>50)	0.029 ± 0.007 (10)
HIV-$1_{MDR/C}$	0.26 ± 0.03 (9)	0.013 ± 0.0004 (4)	>1 (>50)	0.022 ± 0.003 (7)
HIV-$1_{MDR/G}$	0.38 ± 0.03 (12)	0.0023 ± 0.0006 (1)	0.27 ± 0.02 (13)	0.0045 ± 0.0007 (2)
HIV-$1_{MDR/TM}$	0.19 ± 0.06 (6)	0.0019 ± 0.0003 (1)	0.041 ± 0.004 (2)	0.0031 ± 0.002 (1)

[a] Amino acid substitutions identified in the protease-encoding region compared to the consensus type B sequence cited from the Los Alamos database: L10I, L33I, M36I, M46I, F53L, K55R, I62 V, L63P, A71 V, G73S, V82A, L90M, and I93L in HIV-1MDR/B; L10I, I15 V, K20R, L24I, M36I, M46L, I54 V, I62 V, L63P, K70Q, V82A, and L89 M in HIV-1MDR/C; L10I, V11I, T12E, I15 V, L19I, R41K, M46L, L63P, A71T, V82A, and L90 M in HIV-1MDR/G; L10I, K14R, R41K, M46L, I54V, L63P, A71V, V82A, L90M, I93L in HIV-$1_{MDR/TM}$. HIV-$1_{ERS104pre}$ served as a source of wild-type HIV-1. [b] IC_{50} values were determined by using PHA-PBMs as target cells, and inhibition of p24 Gag protein production by each drug was used as an end point. Numbers in parentheses represent *n*-fold changes of IC_{50} for each isolate compared to IC_{50} for the wild-type HIV-$1_{ERS104pre}$. All assays were conducted in duplicate or triplicate, and data shown represent mean values (±1 standard deviation) derived from results of three independent experiments. PHA-PBMs were derived from a single donor in each independent experiment. DRV: darunavir. APV: amprenavir.

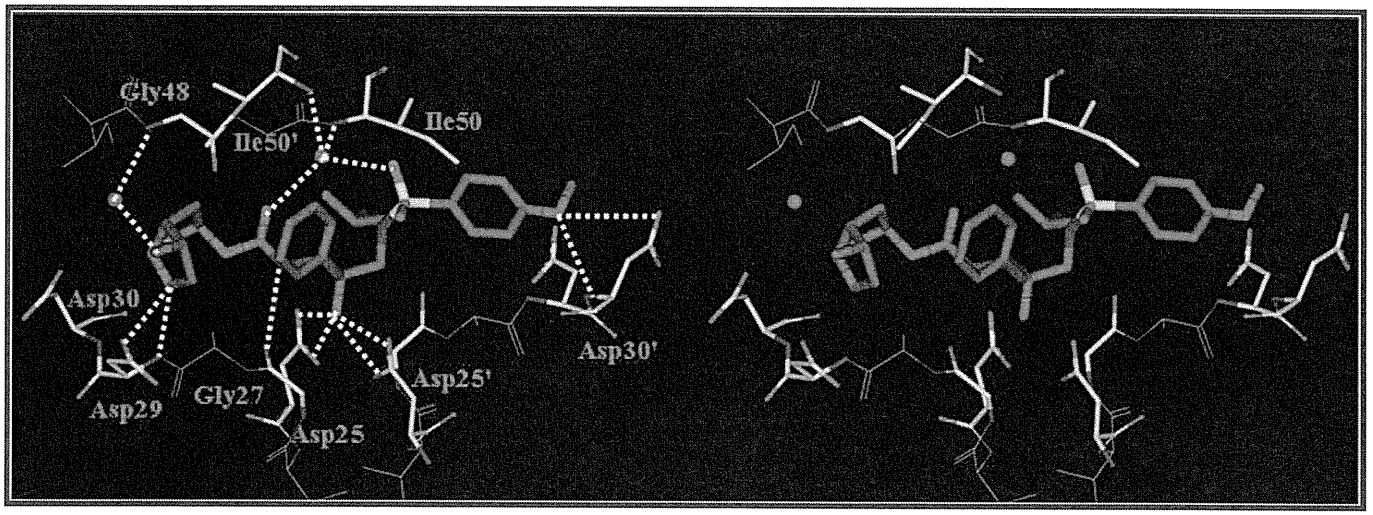

Figure 2. Stereoview of the X-ray structure of inhibitor **26** bound to the active site of the wild-type HIV-1 protease.

related by a 180° rotation with a 0.55/0.45 ratio. The protease backbone structure showed a very low rms deviation of 0.15 Å for all Cα atoms compared to protease complexes of **2** or darunavir.[19,20] The inhibitor makes extensive interactions from the P2 to P2′ ligands with the protease atoms and most notably displays favorable polar interactions including hydrogen bonds, weaker C−H···O and C−H···π interactions, as shown in Figure 2. The central hydroxyl group forms hydrogen bonds with the side chain carboxylate oxygen atoms of the catalytic Asp25 and Asp25′ residues. The inhibitor hydrogen-bonds with the protease backbone atoms of the amide of Asp30′, the carbonyl oxygen of Gly27, and forms water-mediated interactions with the amides of Ile50 and Ile50′, which are generally conserved in the majority of protease complexes with inhibitors[21] or substrate analogues.[22,23] The inhibitor interactions with atoms in the binding cavity resemble those of darunavir and **2** (TMC-126) with the exception of the interactions of the new P2-ligand that replaces the bis-THF group. The 3-(*R*)-hydroxyl of the Cp-THF ligand extends toward the flap region and forms a new water-mediated hydrogen bond interaction with the backbone amide NH of Gly48, with interatomic distances of 2.5 and 3.1 Å for the major inhibitor orientation or 2.7 and 3.1 Å for the minor orientation. Also, the Cp-THF ether oxygen forms a strong hydrogen bond with the backbone amide NH of Asp29. These new interactions with the backbone atoms of Gly48 are likely to be responsible for the impressive antiviral activity and drug resistance properties of this inhibitor. The C3-functionality on the Cp-THF appears to enhance the affinity of the inhibitor. The new water-mediated interaction with the backbone NH of Gly48 on the protease flap may promote thermodynamic stabilization of the closed conformation of the protease−ligand complex. This may slow the kinetics of dissociation of the inhibitor through flexible opening of the protease flap.

CONCLUSION

In summary, we have designed a number of C3-substituted hexahydrocyclopentafuranylurethanes as P2-ligands to enhance interactions with the protein backbone in the S2-subsite. The ligands were stereoselectively synthesized in optically active form. Incorporation of these ligands in (*R*)-hydroxyethylsulfonamide isosteres resulted in a series of novel and highly potent HIV-1 protease inhibitors. In particular, inhibitor **26** displayed remarkable enzyme inhibitory and antiviral potency. Also, inhibitor **26** has shown excellent activity against multi-PI-resistant

variants compared to other FDA approved inhibitors. A protein−ligand X-ray structure of **26**-bound HIV-1 protease was determined at 1.45 Å resolution. The inhibitor appeared to make extensive interactions throughout the active site. Of particular interest, the 3-(*R*)-hydroxyl of the Cp-THF ligand formed a new water-mediated hydrogen bond interaction with the backbone amide NH of Gly48, and the Cp-THF ether oxygen formed a strong hydrogen bond with backbone amide NH of Asp29. The extensive interactions with the protein backbone may be responsible for inhibitor **26**'s impressive antiviral activity and drug resistance profile. The design of inhibitors targeting the protein backbone has led us to develop inhibitors characterized by high potency against both wild-type and multidrug-resistant HIV-1 strains. Further design and optimization of inhibitors utilizing this molecular insight are in progress.

EXPERIMENTAL SECTION

General. All anhydrous solvents were obtained according to the following procedures. Diethyl ether and tetrahydrofuran (THF) were distilled from sodium/benzophenone under argon. Toluene, methanol, acetonitrile, and dichloromethane were distilled from calcium hydride, and benzene was distilled from sodium. Other solvents were used without purification. All moisture-sensitive reactions were carried out in flame-dried flasks under argon atmosphere. Reactions were monitored by thin layer chromatography (TLC) using Silicycle 60A-F254 silica gel precoated plates. Flash column chromatography was performed using Silicycle 230−400 mesh silica gel. Yields refer to chromatographically and spectroscopically pure compounds. Optical rotations were recorded on a Perkin-Elmer 341 polarimeter. ^{1}H NMR and ^{13}C NMR spectra were recorded on a Varian Inova-300 (300 and 75 MHz, respectively), Bruker Avance ARX- 400 (400 and 100 MHz), and Bruker Avance ARX-500 (500 and 125 MHz). High and low resolution mass spectra were carried out by the Mass Spectroscopy Center at Purdue University, IN. The purity of all test compounds was determined by HRMS and HPLC analyses in the different solvent systems. All test compounds showed ≥95% purity.

(3a*S*,5*R*,6a*R*)-5-Hydroxytetrahydro-2*H*-cyclopenta[*b*]furan-3(3a*H*)-one (7). A solution of ketone **6** (23 mg, 0.09 mmol) in CH_3CN (0.5 mL) was cooled to 0 °C under argon. Pyridine (50 μL) was added followed by dropwise addition of HF−pyridine (0.18 mL). The solution was stirred at 0 °C for 4 h. The reaction was quenched by addition of saturated aqueous $NaHCO_3$ solution followed by solid $NaHCO_3$. The aqueous phase was extracted multiple times with EtOAc, and the combined organic layer was dried over Na_2SO_4. Following careful evaporation of the solvent, the residue was purified by column chromatography on silica gel using hexanes/EtOAc (1:1 and then 1:2) as the eluent to yield the desired ketone **7** (12 mg, 94%) as a colorless oil. TLC, R_f = 0.32 (hexanes/EtOAc = 1:2); $[\alpha]_D^{20}$ +96.1 (*c* 0.86, $CHCl_3$); ^{1}H NMR ($CDCl_3$, 400 MHz) δ 5.04 (t, *J* = 6.6 Hz, 1H), 4.38 (t, *J* = 4.0 Hz, 1H), 4.20 (d, *J* = 17.0 Hz, 1H), 3.97 (d, *J* = 17.0 Hz, 1H), 2.85 (t, *J* = 8.4 Hz, 1H), 2.21 (d, *J* = 13.9 Hz, 1H), 2.15 (d, *J* = 15.2 Hz, 1H), 2.01 (ddd, *J* = 3.9, 10.5, 14.1 Hz, 1H), 1.95 (ddd, *J* = 4.5, 6.0, 15.1 Hz, 1H), 1.90 (br s, 1H); ^{13}C NMR ($CDCl_3$, 100 MHz) δ 217.7, 84.0, 72.9, 70.8, 48.8, 43.4, 40.7.

(3*S*,3a*S*,5*R*,6a*R*)-3-Methoxyhexahydro-2*H*-cyclopenta-[*b*]furan-5-ol (8). Ketone **6** (35.6 mg, 0.14 mmol) was dissolved in EtOH (1 mL) under argon and cooled to −25 °C. To the solution was added $NaBH_4$ (10 mg, 0.26 mmol) in one protion, and the resulting mixture was stirred at this temperature for 20 min. Saturated aqueous NH_4Cl solution was added and the volume of solvent reduced under vacuum. Additional water was added, and the aqueous phase was extracted several times with EtOAc. The combined organic layer was washed with brine, dried (Na_2SO_4), and evaporated in vacuo. Purification of the crude alcohol by column chromatography on silica gel using hexanes/EtOAc (5:1) as the eluent provided the corresponding alcohol (32.2 mg, 90%) as a colorless oil. TLC, R_f = 0.22 (hexanes/EtOAc = 5:1); $[\alpha]_D^{20}$ +21.5 (*c* 1.05, $CHCl_3$); ^{1}H NMR ($CDCl_3$, 300 MHz) δ 4.55 (br s, 1H), 4.42 (t, *J* = 7.0 Hz, 1H), 4.34 (t, *J* = 4.5 Hz, 1H), 4.11 (m, 1H), 3.87 (d, *J* = 9.9 Hz, 1H), 3.48 (dd, *J* = 3.6, 9.9 Hz, 1H), 2.89 (dt, *J* = 7.8, 10.2 Hz, 1 H), 2.13 (dd, *J* = 2.4, 14.7 Hz, 1H), 1.99 (dd, *J* = 2.4, 14.7 Hz, 1H), 1.78−1.65 (m, 2 H), 0.89 (s, 9H), 0.11 (s, 3H), 0.10 (s, 3H); ^{13}C NMR ($CDCl_3$, 75 MHz) δ 85.3, 77.3, 74.9, 72.9, 48.1, 41.8, 34.8, 25.7, 18.0, −4.7, −5.2. HRMS-CI (*m*/*z*): $[M + H]^+$ calcd for $C_{13}H_{27}O_3Si$ 259.1729, found 259.1731. To a solution of the above alcohol (27 mg, 0.1 mmol) in CH_3CN (1 mL) was added MeI (0.3 mL, excess) followed by Ag_2O (50 mg, 0.2 mmol). The mixture was gently refluxed for 12 h under argon, and then additional MeI (0.3 mL) and Ag_2O (50 mg) were added. Reflux was continued for an additional 12 h until all SM disappeared. The resulting mixture was diluted in Et_2O and filtered on Celite. After evaporation of the solvent, the residue was purified by column chromatography on silica gel using hexanes/EtOAc (8:1) as the eluent to yield the corresponding 3-(*S*)-methoxy intermediate as a clear oil (23 mg, 85%). TLC, R_f = 0.38 (hexanes/EtOAc = 5:1); $[\alpha]_D^{20}$ +42.6 (*c* 1.02, $CHCl_3$); ^{1}H NMR ($CDCl_3$, 300 MHz) δ 4.41 (dt, *J* = 5.1, 7.2 Hz, 1H), 4.12 (m, 1H), 3.93 (m, 1H), 3.87−3.70 (m, 2H), 3.32 (s, 3H), 2.61 (m, 1H), 2.18 (m, 1H), 1.90−1.75 (m, 2H), 1.63 (m, 1H), 0.88 (s, 9H), 0.05 (s, 6H); ^{13}C NMR ($CDCl_3$, 75 MHz) δ 82.5, 81.1, 73.5, 69.0, 57.8, 42.6, 33.5, 25.8, 18.1, −4.8. To a solution of the above intermediate (16 mg, 0.059 mmol) in THF (1 mL) was added TBAF (1 M solution in THF, 0.1 mmol, 100 μL). The solution was stirred at room temperature for 2 h. The solvent was evaporated and the residue purified by flash column chromatography on silica gel using hexanes/EtOAc (1:1 and then 1:2.5) to furnish **8** as a colorless oil (8 mg, 86%). TLC, R_f = 0.32 ($CHCl_3$/3% EtOH); ^{1}H NMR ($CDCl_3$, 500 MHz) δ 4.41 (t, *J* = 4.4 Hz, 1H), 4.21 (dt, *J* = 5.1, 10.1 Hz, 1H), 4.08 (d, *J* = 10.3 Hz, 1H), 3.85 (dd, *J* = 3.0, 7.3 Hz, 1H), 3.83 (d, *J* = 10.3 Hz, 1H), 3.42 (s, 3H), 2.94−2.86 (m, 1H), 2.13 (d, *J* = 14.5 Hz, 1H), 2.08 (dd, *J* = 2.4, 15.1 Hz, 1H), 1.81 (ddd, *J* = 5.3, 10.6, 14.5 Hz, 1H), 1.74 (ddd, *J* = 5.3, 6.0, 15.0 Hz, 1H); ^{13}C NMR ($CDCl_3$, 125 MHz) δ 86.0, 82.1, 73.6, 71.6, 57.4, 47.2, 42.0, 34.0.

Methyl 2-{(1*R*,4*S*)-4-[(*tert*-Butyldimethylsilyl)oxy]cyclopent-2-en-1-yloxy}acetate (9). To an ice-cold suspension of NaH (60% suspension in oil, 360 mg, 9 mmol) in dry THF (5 mL) under argon was slowly added a solution of 2-bromoacetic acid (520 mg, 3.75 mmol) in dry THF (3 mL + 3 mL rinse). The resulting mixture was stirred at room temperature for 30 min and then cooled back to 0 °C. Desymmetrized *meso*-cyclopentenediol **5** (642 mg, 3 mmol) in dry DMF (10 mL) was slowly added to this solution, and the mixture was allowed to warm to room temperature and was stirred for 24 h. A pH 4 phosphate buffer solution was added at 0 °C, and the aqueous phase was extracted with EtOAc (×4). The combined organic phase was dried (Na_2SO_4), filtered, and evaporated in vacuo to give the corresponding crude carboxylic acid along with residual DMF. The acid was diluted with additional DMF (10 mL). The solution was cooled to 0 °C, and $NaHCO_3$ (630 g, 7.5 mmol) was added at once followed by MeI (14 mmol, 1.98 g, 871 μL). After the mixture was stirred at room temperature for 12 h, saturated aqueous NH_4Cl solution was added (10 mL), then water (10 mL), and the aqueous phase was successively extracted with hexanes/Et_2O, 1:1 (×3). The combined organic phase was dried (Na_2SO_4), filtered, and evaporated. The residue was purified by flash chromatography on silica gel using hexanes/EtOAc (20:1 and then 15:1) to give methyl ester **9** as a colorless oil (654 mg, 76%, two steps). TLC, R_f = 0.45 (hexanes/EtOAc = 3:1); ^{1}H NMR ($CDCl_3$, 300 MHz) δ 5.92 (s, 2H), 4.63 (dd, *J* = 4.8, 7.0 Hz, 1H), 4.53 (dd, *J* = 5.1, 7.2 Hz, 1H), 4.10 (s, 2H), 3.74 (s, 3H), 2.64 (dt, *J* = 7.2, 13.8 Hz, 1H), 1.60 (dt, *J* = 4.9, 13.7 Hz, 1H), 0.87 (s, 9H), 0.065 (s, 3H), 0.06 (s, 3H); ^{13}C NMR ($CDCl_3$, 75 MHz) δ 171.2, 138.4, 131.9, 82.4, 74.6, 64.7, 51.8, 40.5, 25.8, 18.0, −4.7.

(3*R*,3a*R*,5*R*,6a*R*)-5-[(*tert*-Butyldimethylsilyl)oxy]hexahydro-2*H*-cyclopenta[*b*]furan-3-ol (10). A solution of methyl ester **9** (87.2 mg,

0.304 mmol) in dry CH_2Cl_2 (8 mL) was cooled to −78 °C under argon. DIBAL-H (1 M solution in hexanes, 0.40 mL) was added slowly, and the reaction mixture was stirred for 1 h at this temperature. The reaction was quenched by addition of MeOH (100 μL), and the mixture was warmed to room temperature. A pH 7 phosphate buffer (0.5 M solution, 2 mL) was added. The aqueous phase was extracted with CH_2Cl_2 (×3) and the combined organic phase washed with brine, dried (Na_2SO_4), filtered, and evaporated in vacuo. The crude aldehyde solution was passed through a short plug of silica gel, deactivated with 1% Et_3N using hexanes/EtOAc (5:1) as the eluent. After evaporation, the crude product was directly submitted to the next step. The residue was dissolved in dry benzene (degassed, 2 mL) under argon and the solution transferred into a sealable tube. $(n\text{-}Bu_3Sn)_2O$ (22.5 μL, 26.3 mg, 44 μmol), Ph_2SiH_2 (42 μL, 41.6 mg, 0.22 mmol), EtOH (45 μL), and AIBN (10 mg) were successively added. The sealed tube was placed with stirring in an oil bath at 80 °C for 6 h. After cooling to room temperature, the reaction mixture was diluted with Et_2O (2 mL) and aqueous 0.5 M HCl solution (2 mL) was added. After the mixture was stirred at room temperature for 15 min, the aqueous phase was extracted with Et_2O (×3). The combined organic phase was washed with saturated aqueous $NaHCO_3$ solution, brine, dried ($MgSO_4$), filtered, and evaporated. The residue was purified by flash chromatography on silica gel using hexanes/EtOAc (6:1 to 2:1) to afford the (*R*)-alcohol **10** (50 mg, 64%, over two steps) as a white solid; 5 mg of the other 3-(*S*)-diastereoisomer was also isolated, and only traces of 1,2 reduction product was observed. TLC, R_f = 0.46 (hexanes/EtOAc = 3:1); $[\alpha]_D^{20}$ +22.3 (*c* 0.67, $CHCl_3$); ^{1}H NMR ($CDCl_3$, 300 MHz) δ 4.69 (dt, *J* = 3.8, 7.2 Hz, 1H), 4.19−4.02 (m, 3H), 3.72 (d, *J* = 9.8 Hz, 1H), 2.48 (q, *J* = 7.5 Hz, 1H), 2.13−1.96 (m, 2H), 1.70−1.55 (m, 1H), 1.47−1.25 (m, 1H), 0.86 (s, 9H), 0.03 (s, 6H); ^{13}C NMR ($CDCl_3$, 75 MHz) δ 82.2, 78.3, 73.1, 72.7, 50.9, 42.4, 39.0, 25.8, 17.5, −4.8, −4.9.

(3*R*,3a*S*,5*R*,6a*R*)-5-Hydroxyhexahydro-2*H*-cyclopenta-[*b*]furan-3-yl Acetate (11). Alcohol **10** (45 mg, 0.175 mmol) was diluted in CH_2Cl_2 (5 mL), and the solution was cooled to 0 °C under argon. Et_3N (0.525 mmol, 53 mg, 75 μL) and DMAP (1 crystal) were added followed by acetic anhydride (25 μL, 0.23 mmol). The mixture was warmed to room temperature and stirred overnight. The solution was evaporated to dryness, and purification of the residue by flash column chromatography on silica gel using hexanes/EtOAc (20:1) furnished the corresponding acetate derivative (38 mg, 73%). TLC, R_f = 0.24 (hexanes/EtOAc = 10:1); ^{1}H NMR ($CDCl_3$, 300 MHz) δ 5.02 (d, *J* = 3.8 Hz, 1H), 4.69 (dt, *J* = 3.2, 7.2 Hz, 1H), 4.22 (dd, *J* = 4.0, 10.4 Hz, 1H), 4.11 (m, 1H), 3.80 (d, *J* = 10.4 Hz, 1H), 2.56 (m, 1H), 2.09−1.97 (m, 2H), 2.04 (s, 3H), 1.71 (m, 1H), 1.68−1.54 (m, 1H), 0.86 (s, 9H), 0.03 (s, 6H); ^{13}C NMR ($CDCl_3$, 75 MHz) δ 170.8, 82.9, 81.2, 72.8, 70.9, 48.5, 42.7, 39.2, 25.8, 21.2, 18.0, −4.9. The acetate (28 mg, 0.093 mmol) was diluted in THF (1.5 mL). TBAF (1 M solution of THF, 200 μL, 0.2 mmol) was added at 0 °C, and the mixture was stirred for 2.5 h while warming to 23 °C. The solvent was evaporated and the residue purified by flash column chromatography on silica gel using hexanes/EtOAc (3:1 to 1:1) to give pure alcohol **11** as a colorless oil (17.5 mg, quant). TLC, R_f = 0.18 (EtOAc, 100%); ^{1}H NMR ($CDCl_3$, 300 MHz) δ 5.11 (m, 1H), 4.70−4.62 (m, 1H), 4.32 (dd, *J* = 5.0, 10.4 Hz, 1H), 4.28−4.20 (m, 1H), 3.71 (dd, *J* = 3.2, 10.4 Hz, 1H), 2.65−2.56 (m, 1H), 2.30−2.13 (m, 2H), 2.06 (s, 3H), 1.99−1.88 (m, 1H), 1.77−1.68 (m, 1H); ^{13}C NMR ($CDCl_3$, 75 MHz) δ 170.8, 84.8, 81.1, 73.4, 71.9, 48.9, 41.9, 39.5, 21.1.

(3*R*,3a*S*,5*R*,6a*R*)-3-Methoxyhexahydro-2*H*-cyclopenta-[*b*]furan-5-ol (12). A solution of alcohol **10** (30 mg, 0.116 mmol) in dry DMF (1 mL) was cooled to 0 °C under argon, and NaH (60% suspension in oil, 15 mg, 0.348 mmol) was added in one portion. The mixture was warmed to room temperature, stirred for 30 min, and then cooled to 0 °C. MeI (22 μL, 50 mg, 0.35 mmol) was added to the solution, and the mixture was warmed to 23 °C and stirred for 3.5 h. Saturated aqueous NH_4Cl solution was added, and the aqueous phase was extracted with Et_2O/hexanes (1:1). The combined organic phase was washed with brine, dried (Mg_2SO_4), filtered, and evaporated in vacuo. The residue was purified by flash chromatography on silica gel using hexanes/EtOAc (10:1 and then 8:1) to afford the corresponding TBS-protected methoxy compound (28.6 mg, 86%) as a clear oil. TLC, R_f = 0.61 (hexanes/EtOAc = 3:1); $[\alpha]_D^{20}$ +20.6 (*c* 1.52, $CHCl_3$); ^{1}H NMR ($CDCl_3$, 400 MHz) δ 4.63 (dt, *J* = 3.6, 7.2 Hz, 1H), 4.11 (m, 1H), 4.05 (dd, *J* = 4.1, 9.9 Hz, 1H), 3.81 (dd, *J* = 1.3, 9.9 Hz, 1H), 3.74 (m, 1H), 3.31 (s, 3H), 2.54 (td, *J* = 7.7, 8.3 Hz, 1H), 2.10−1.96 (m, 2H), 1.70−1.60 (m, 1H), 1.47 (m, 1H), 0.87 (s, 9H), 0.04 (6H); ^{13}C NMR ($CDCl_3$, 100 MHz) δ 87.7, 82.5, 72.9, 70.3, 56.6, 47.4, 42.5, 39.5, 25.8, 18.0, −4.8, −4.9. To an ice-cold solution of the above methoxy intermediate (27 mg, 0.1 mmol) in THF (2 mL) under argon was added TBAF (1 M solution in THF, 0.2 mL, 0.2 mmol). The mixture was stirred for 1.5 h. The solvent was evaporated, and the crude residue was purified by flash column chromatography on silica gel using hexanes/EtOAc (1:1) as the eluent to furnish alcohol **12** as a clear oil (13 mg, 82%). TLC, R_f = 0.17 (hexanes/EtOAc = 1:2); ^{1}H NMR ($CDCl_3$, 300 MHz) δ 4.63 (t, *J* = 5.5 Hz, 1H), 4.26 (m, 1H), 4.20 (dd, *J* = 5.3, 9.7 Hz, 1H), 3.89 (dt, *J* = 2.0, 4.8 Hz, 1H), 3.65 (dd, *J* = 4.4, 9.7 Hz, 1H), 3.34 (s, 3H), 2.64−2.54 (m, 1H), 2.40 (br s, 1H), 2.16 (ddd, *J* = 5.5, 10.6, 14.3 Hz, 1H), 2.02 (dd, *J* = 1.7, 14.7 Hz, 1H), 1.87 (dt, *J* = 5.1, 14.7 Hz, 1H), 1.77−1.61 (m, 1H); ^{13}C NMR ($CDCl_3$, 75 MHz) δ 88.4, 85.1, 74.0, 71.9, 57.0, 48.4, 41.8, 40.2.

(3*S*,3a*R*,5*R*,6a*R*)-3-Methylhexahydro-2*H*-cyclopenta[*b*]furan-5-ol (14). To a solution of olefin **13** (29.7 mg, 0.12 mmol) in toluene (3 mL) was added Wilkinson's catalyst, $RhCl(PPh_3)_3$ (18 μmol, 17 mg). The resulting solution was then placed under a hydrogen atmosphere and stirred for 3 h. After dilution with additional toluene, the solution was filtered on a Celite pad, and the pad was rinsed with toluene. Evaporation of the solvent and purification of the residue on silica gel using hexanes/EtOAc (100:1 and then 50:1) as the eluent furnished the corresponding 3-(*S*)-methyl compound (29 mg, 97%). TLC, R_f = 0.28 (hexanes/EtOAc = 20:1); $[\alpha]_D^{20}$ +22.7 (*c* 1.01, $CHCl_3$); ^{1}H NMR ($CDCl_3$, 400 MHz) δ 4.43 (m, 1H), 4.03 (m, 1H), 3.81 (dd, *J* = 7.4, 8.0 Hz, 1H), 3.42 (dd, *J* = 8.0, 10.7 Hz, 1H), 2.43 (m, 1H), 2.32−2.18 (m, 2H), 1.72 (m, 1H), 1.51 (ddd, *J* = 4.8, 8.6, 13.5 Hz, 1H), 1.44 (m, 1H), 0.95 (d, *J* = 6.8 Hz, 3H), 0.88 (s, 9H), 0.05 (s, 6H); ^{13}C NMR ($CDCl_3$, 100 MHz) δ 82.6, 73.2, 71.6, 44.5, 43.2, 36.2, 34.7, 25.9, 18.2, 11.3, −4.7, −4.8. HRMS-CI (*m*/*z*): $[M + H]^+$ calcd for $C_{14}H_{29}O_2Si$ 257.1937, found 257.1936. A solution of methyl-based ligand (28 mg, 0.1 mmol) in THF (2 mL) was treated with TBAF (1 M solution in THF, 150 μL) and stirred at room temperature for 2.5 h. The reaction mixture was diluted with Et_2O and filtered on a short silica pad. The solvent containing the alcohol was carefully reduced, and essentially pure alcohol **14** was directly used in the next step without purification (>99% pure). TLC, R_f = 0.26 (hexanes/EtOAc = 1:1); ^{1}H NMR ($CDCl_3$, 400 MHz) δ 4.46 (dt, *J* = 2.7, 5.5 Hz, 1H), 4.20 (m, 1H), 3.88 (t, *J* = 7.8 Hz, 1H), 3.48 (t, *J* = 9.2 Hz, 1H), 2.59−2.40 (m, 2H), 2.22 (d, *J* = 6.9 Hz, 1H), 2.08 (dt, *J* = 5.9, 14.1 Hz, 1H), 1.87 (ddd, *J* = 6.0, 9.5, 13.7 Hz, 1H), 1.83 (m, 1H), 1.68−1.54 (m, 1H), 1.01 (d, *J* = 6.8 Hz, 3H); ^{13}C NMR ($CDCl_3$, 100 MHz) δ 85.3, 73.8, 72.9, 46.3, 42.4, 36.5, 34.5, 12.7.

(3*R*,3a*R*,6a*R*)-3-Methyl-3,3a,6,6a-tetrahydro-2*H*-cyclopenta-[*b*]furan-2-one (16). To a solution of lithium diisopropylamide, prepared by adding *n*-BuLi (2.5 M solution in hexanes, 1.36 mL, 3.39 mmol) to diisopropylamine (477 μL, 3.39 mmol) in THF (15 mL) at 0 °C, was added a precooled solution of known (3a*S*,6a*R*)-3,3a,6,6a-tetrahydro-2*H*-cyclopenta[*b*]furan-2-one (+)-**15** (350 mg, 2.82 mmol) in THF (5 mL + 3 mL rinse) at −78 °C, dropwise. The reaction mixture was stirred at this temperature for 30 min. Then methyl iodide (352 μL, 5.65 mmol) was added dropwise and the reaction mixture was stirred at −78 °C for 6 h. The reaction mixture was quenched with 2 M aqueous HCl. The aqueous phase was extracted with Et_2O (×3). The combined organic layer was dried (Na_2SO_4), filtered, and concentrated under vacuum. The residue was purified by column chromatography on silica gel using hexanes/Et_2O (5:1)

to yield lactone **16** (369 mg, 95%) as a brown oil. TLC, R_f = 0.54 (hexanes/EtOAc = 2:1); $[\alpha]_D^{20}$ +54.2 (*c* 1.0, $CHCl_3$); ^1H NMR ($CDCl_3$, 400 MHz) δ 5.74 (m, 1H), 5.59 (m, 1H), 5.12 (t, *J* = 5.6 Hz, 1H), 3.13 (dd, *J* = 3.8, 1.8 Hz, 1H), 2.65 (m, 2H), 2.52 (q, *J* = 7.6 Hz, 1H), 1.33 (d, *J* = 7.6 Hz, 3H); ^{13}C NMR ($CDCl_3$, 100 MHz) δ 180.0, 130.9, 129.4, 81.3, 53.8, 39.9, 39.2, 17.4.

(3*R*,3a*R*,5*R*,6a*R*)-5-Hydroxy-3-methylhexahydro-2*H*-cyclopenta[*b*]furan-2-one (17). To an ice-cold yellow solution of $Hg(OAc)_2$ (1.45 g, 4.57 mmol) in THF/H_2O (2.5:1 ratio, 23 mL) was added perchloric acid (~0.7 mL) until the solution became colorless. A solution of lactone **16** (350 mg, 2.54 mmol) in THF (7 mL) was then added at 0 °C, and the mixture was stirred for 1 h. Additional $Hg(OAc)_2$ (646 mg, 2.03 mmol) similarly pretreated with perchloric acid in THF/H_2O (2.5:1, 10 mL) was added, and stirring was continued for 2 h at 0 °C. The pH of the mixture was then adjusted to ~10 by addition of a 1 M aqueous NaOH solution. Stirring was then continued for 1 h at room temperature. The solution was cooled to 0 °C, and $NaBH_4$ (145 mg, 3.81 mmol) was added in small portions. After 1 h, the reaction mixture was acidified to pH 2 with concentrated HCl, and stirring was continued for 1 h. The reaction solution was saturated with NaCl and the aqueous phase extracted several times with EtOAc. The combined organic phase was dried (Na_2SO_4), filtered, and concentrated under vacuum. The residue was purified by column chromatography on silica gel using 2% MeOH in CH_2Cl_2 to yield alcohol **17** (252 mg, 64%) as a colorless oil. TLC, R_f = 0.31 ($CHCl_3$/MeOH = 9/1); $[\alpha]_D^{20}$ +53.5 (*c* 1.0, $CHCl_3$); ^1H NMR ($CDCl_3$, 400 MHz) δ 4.98 (dt, *J* = 8.0, 14.9 Hz, 1H), 4.55 (m, 1H), 2.69 (qd, *J* = 3.9, 7.6 Hz, 1H), 2.58 (m, 1H), 2.55 (m, 1H), 2.09 (d, *J* = 15.0 Hz, 1H), 1.94 (m, 2H), 1.83 (m, 1H), 1.26 (d, *J* = 7.6 Hz, 3H); ^{13}C NMR ($CDCl_3$, 100 MHz) δ 181.0, 83.8, 74.6, 51.2, 45.5, 43.9, 41.3, 18.4.

(3*R*,3a*R*,5*R*,6a*R*)-3-Methylhexahydro-2*H*-cyclopenta[*b*]furan-5-ol (18). To a solution of lactone **17** (205 mg, 1.31 mmol) in CH_2Cl_2 (9 mL) was added DIBAL-H (1 M solution in CH_2Cl_2, 1.45 mL, 1.45 mmol) dropwise at −78 °C. The mixture was stirred for 3 h and then quenched with saturated Rochelle's salt solution. After the mixture was stirred overnight at room temperature, the phases were separated and the aquoues phase was extracted with EtOAc (×3). The combined organic phase was dried (Na_2SO_4), filtered, and concentrated under reduced pressure. The residue was purified by column chromatography on silica gel using 2% MeOH in CH_2Cl_2 to yield the corresponding lactol (150 mg, 72%). To a solution of this lactol (143 mg, 0.9 mmol) in CH_2Cl_2 (9 mL) at −78 °C was added $TiCl_4$ (100 μL, 0.9 mmol) dropwise, and the mixture was stirred for 20 min. Et_3SiH (289 μL, 1.81 mmol) was then added, and the solution was stirred for an additional 1 h. The reaction was quenched with saturated $NaHCO_3$ solution once completion was reached as observed by TLC. The aqueous phase was extracted with Et_2O, dried (Na_2SO_4), filtered, and concentrated under reduced pressure at 25 °C. The residue was purified by column chromatography on silica gel using 2% MeOH in CH_2Cl_2 to yield alcohol **18** (122 mg, 95%) as a colorless oil. TLC, R_f = 0.38 ($CHCl_3$/MeOH = 9/1); $[\alpha]_D^{20}$ +12.6 (*c* 1.0, $CHCl_3$); ^1H NMR ($CDCl_3$, 400 MHz) δ 4.47 (t, *J* = 5.7 Hz, 1H), 4.22 (m, 1H), 4.06 (dd, *J* = 6.5, 8.7 Hz, 1H), 3.18 (t, *J* = 8.4 Hz, 1H), 2.60 (d, *J* = 7.2 Hz, 1H), 2.27−2.18 (m, 1H), 2.18−2.12 (m, 1H), 2.00 (dd, *J* = 1.5, 16.2 Hz, 1H), 1.98−1.91 (m, 1H), 1.80 (dt, *J* = 5.2, 14.6 Hz, 1H), 1.69 (ddd, *J* = 2.3, 5.4, 13.9 Hz, 1H), 1.03 (d, *J* = 6.7 Hz, 3H); ^{13}C NMR ($CDCl_3$, 100 MHz) δ 85.4, 75.1, 74.7, 50.3, 43.2, 41.6, 41.5, 17.6.

Synthesis of Activated Mixed Carbonates. (3a*S*,5*R*,6a*R*)-3-Oxohexahydro-2*H*-cyclopenta[*b*]furan-5-yl (4-nitrophenyl)carbonate (19a). To a solution of ketone **7** (20 mg, 0.14 mmol) in CH_2Cl_2 (1 mL) was added pyridine (30 μL). The solution was cooled to 0 °C under argon, and 4-nitrophenyl chloroformate (42 mg, 0.21 mmol) was added at once. A white suspension formed. The solution was stirred at this temperature and slowly warmed to room temperature until all starting material was consumed. The reaction mixture was evaporated to dryness and the residue purified by column chromatography on silica gel using hexanes/EtOAc (3:1 and then 2:1) as eluent to furnish pure mixed carbonate **19a** (39 mg, 92%) as a white solid. TLC, R_f = 0.25 (hexanes/EtOAc = 2:1); ^1H NMR ($CDCl_3$, 400 MHz) δ 8.27 (d, *J* = 9.2 Hz, 2H), 7.34 (d, *J* = 9.2 Hz, 2H), 5.23 (t, *J* = 4.2 Hz, 1H), 5.13 (t, *J* = 6.9 Hz, 1H), 4.19 (d, *J* = 17.1 Hz, 1H), 4.06 (d, *J* = 17.1 Hz, 1H), 2.99 (dd, *J* = 8.7, 8.8 Hz, 1H), 2.54−2.41 (m, 2H), 2.22−2.08 (m, 2H); ^{13}C NMR ($CDCl_3$, 100 MHz) δ 216.8, 155.3, 151.5, 145.4, 125.3, 121.9, 82.4, 81.0, 70.6, 48.5, 41.2, 37.1.

(3*S*,3a*S*,5*R*,6a*R*)-3-Methoxyhexahydro-2*H*-cyclopenta[*b*]-furan-5-yl (4-nitrophenyl)carbonate (19b). The title compound was obtained from **8** in 82% yield as described for **7** after purification by column chromatography on silica gel using hexanes/EtOAc (3:1 to 2:1) as the eluent (white solid). TLC, R_f = 0.25 (hexanes/EtOAc = 2:1); ^1H NMR ($CDCl_3$, 300 MHz) δ 8.27 (d, *J* = 9.2 Hz, 2H), 7.38 (d, *J* = 9.2 Hz, 2H), 5.15 (tt, *J* = 4.5, 6.2 Hz, 1H), 4.56 (dt, *J* = 2.8, 6.1 Hz, 1H), 4.04 (dt, *J* = 6.3, 7.5 Hz, 1H), 3.87 (*AB*, dd, *J* = 5.2, 9.1 Hz, 1H), 3.86 (*AB*, dd, *J* = 6.6, 9.1 Hz, 1H), 3.34 (s, 3H), 2.83 (m, 1H), 2.38−2.02 (m, 4H); ^{13}C NMR ($CDCl_3$, 75 MHz) δ 155.6, 152.1, 145.2, 125.2, 121.8, 83.7, 81.4, 77.2, 70.3, 57.9, 44.2, 39.6, 30.2.

(3*R*,3a*S*,5*R*,6a*R*)-5-((4-Nitrophenoxy)carbonyloxy)hexahydro-2*H*-cyclopenta[*b*]furan-3-yl Acetate (19c). The title compound was obtained from **11** in 96% yield as described for **7** after purification by column chromatography on silica gel using hexanes/EtOAc (6:1 and then 4:1) as the eluent (white solid). TLC, R_f = 0.26 (hexanes/EtOAc = 3:1); ^1H NMR ($CDCl_3$, 300 MHz) δ 8.27 (d, *J* = 9.1 Hz, 2H), 7.37 (d, *J* = 9.1 Hz, 2H), 5.20−5.12 (m, 1H), 5.12−5.08 (m, 1H), 4.76 (dt, *J* = 2.0, 6.0 Hz, 1H), 4.27 (dd, *J* = 4.6, 10.4 Hz, 1H), 3.80 (dd, *J* = 2.5, 10.4 Hz, 1H), 2.79−2.70 (m, 1H), 2.37 (ddd, *J* = 6.0, 10.2, 15.0 Hz, 1H), 2.29−2.19 (m, 1H), 2.15 (dt, *J* = 5.6, 15.6 Hz, 1H), 2.07 (s, 3H), 2.02−1.92 (m, 1H); ^{13}C NMR ($CDCl_3$, 75 MHz) δ 170.7, 155.4, 151.9, 145.3, 125.3, 121.8, 83.2, 81.0, 80.5, 71.7, 48.8, 39.6, 35.9, 21.1.

(3*R*,3a*S*,5*R*,6a*R*)-3-Methoxyhexahydro-2*H*-cyclopenta[*b*]-furan-5-yl (4-Nitrophenyl)carbonate (19d). The title was obtained from **12** in 93% yield as described for **7** after purification by column chromatography on silica gel using hexanes/EtOAc (6:1 to 4:1) as the eluent (white solid). TLC, R_f = 0.40 (hexanes/EtOAc = 3:1); ^1H NMR ($CDCl_3$, 400 MHz) δ 8.27 (d, *J* = 9.2 Hz, 2H), 7.37 (d, *J* = 9.2 Hz, 2H), 5.19−5.12 (m, 1H), 4.74−4.67 (m, 1H), 4.13 (dd, *J* = 5.4, 5.5 Hz, 1H), 3.84−3.78 (m, 2H), 3.35 (s, 3H), 2.75−2.68 (m, 1H), 2.36 (ddd, *J* = 6.1, 10.0, 14.8 Hz, 1H), 2.25−2.11 (m, 2H), 1.82 (dddd, *J* = 1.2, 3.8, 5.5, 14.7 Hz, 1H); ^{13}C NMR ($CDCl_3$, 100 MHz) δ 155.5, 151.9, 145.3, 125.3, 121.8, 87.5, 83.0, 81.3, 71.3, 56.9, 48.2, 39.4, 36.2.

(3*S*,3a*R*,5*R*,6a*R*)-3-Methylhexahydro-2*H*-cyclopenta[*b*]-furan-5-yl (4-Nitrophenyl)carbonate (19e). The title compound was obtained from **14** in 83% yield as described for **7** after purification by column chromatography on silica gel using hexanes/EtOAc (10:1 and then 7:1) as the eluent (white solid). TLC, R_f = 0.25 (hexanes/EtOAc = 3:1); ^1H NMR ($CDCl_3$, 300 MHz) δ 8.27 (d, *J* = 9.0 Hz, 2H), 7.37 (d, *J* = 9.0 Hz, 2H), 5.09 (m, 1H), 4.57 (dt, *J* = 2.8, 6.2 Hz, 1H), 3.93 (t, *J* = 8.1 Hz, 1H), 3.51 (dd, *J* = 8.1, 10.4, 1H), 2.65 (m, 1H), 2.46 (m, 1H), 2.38 (m, 1H), 2.11 (m, 1H), 2.02 (ddd, *J* = 2.7, 5.5, 14.8 Hz, 1H), 1.81 (m, 1H), 1.02 (d, *J* = 6.9 Hz, 3H); ^{13}C NMR ($CDCl_3$, 75 MHz) δ 155.5, 152.0, 145.3, 125.3, 121.8, 83.4, 80.8, 72.3, 45.8, 39.7, 36.5, 31.0, 11.8.

(3*R*,3a*R*,5*R*,6a*R*)-3-Methylhexahydro-2*H*-cyclopenta[*b*]-furan-5-yl (4-Nitrophenyl)carbonate (19f). The title compound was obtained from **18** in 50% yield as described for **7** following column chromatography on silica gel using hexanes/EtOAc (10:1 and then 7:1) as the eluent (white solid). TLC, R_f = 0.29 (hexanes/EtOAc = 3:1); $[\alpha]_D^{20}$ +40.6 (*c* 1.0, $CHCl_3$); ^1H NMR ($CDCl_3$, 400 MHz) δ 8.26 (d, *J* = 9.3 Hz, 2H), 7.39 (d, *J* = 9.3 Hz, 2H), 5.19−5.12 (m, 1H), 4.57 (dt, *J* = 2.0, 6.8 Hz, 1H), 4.07 (dd, *J* = 6.3, 8.6 Hz, 1H), 3.31 (dd, *J* = 7.1, 8.6 Hz, 1H), 2.35−2.25 (m, 1H), 2.23−2.17 (m, 2H), 2.17−2.07 (m, 2H), 1.88 (ddd, *J* = 3.8, 5.3, 14.5 Hz, 1H), 1.05 (d, *J* = 6.8 Hz, 3H); ^{13}C NMR

($CDCl_3$, 100 MHz) δ 155.6, 151.9, 145.2, 125.2, 121.8, 83.3, 82.2, 74.9, 50.4, 41.8, 39.5, 37.3, 17.5.

General Method for the Synthesis of HIV-Protease Inhibitors. (3a*S*,5*R*,6a*R*)-3-Oxohexahydro-2*H*-cyclopenta[*b*]furan-5-yl [(2*S*,3*R*)-3-Hydroxy-4-(*N*-isobutyl-4-methoxyphenylsulfonamido)-1-phenylbutan-2-yl]carbamate (21). The *N*-Boc-protected isostere **20a** (82 mg, 0.16 mmol) was dissolved in a 2:1 mixture CH_2Cl_2/TFA and stirred at room temperature for 2 h. The solution was then evaporated and dried in vacuo. The residue was redissolved in CH_3CN (1 mL) and the solution cooled down to 0 °C under argon. Et_3N (100 μL) was added followed by a solution of activated carbonate **19a** (40 mg, 0.13 mmol) in THF (1 mL). The solution was stirred for 36 h and the solution evaporated in vacuo. The residue was purified by column chromatography on silica gel using hexanes/EtOAc (3:1 to 1.5:1) as the eluent to furnish inhibitor **21** (46 mg, 61%) as a white solid. TLC, R_f = 0.23 (hexanes/EtOAc = 1:1); ^{1}H NMR ($CDCl_3$, 500 MHz) δ 7.70 (d, J = 8.8 Hz, 2H), 7.34–7.28 (m, 2H), 7.25–7.19 (m, 3H), 6.98 (d, J = 8.8 Hz, 2H), 5.03 (t, J = 6.9 Hz, 1H), 4.99 (m, 1H), 4.71 (d, J = 8.7 Hz, 1H), 3.97 (s, 2H), 3.87 (s, 3H), 3.89–3.85 (m, 1H), 3.83–3.70 (m, 2H), 3.09 (dd, J = 8.0, 15.2 Hz, 1H), 3.00 (dd, J = 3.0, 15.1 Hz, 1H), 2.99–2.89 (m, 3H), 2.89–2.82 (m, 1H), 2.79 (dd, J = 6.8, 13.4 Hz, 1H), 2.24–2.12 (m, 2H), 2.06–1.94 (m, 2H), 1.81 (m, 1H), 0.90 (d, J = 6.4 Hz, 3H), 0.86 (d, J = 6.4 Hz, 3H); ^{13}C NMR ($CDCl_3$, 125 MHz) δ 216.2, 163.0, 155.4, 137.5, 129.8, 129.6, 129.5, 128.5, 126.6, 114.3, 82.9, 76.3, 72.2, 70.6, 58.8, 55.6, 55.1, 53.7, 48.7, 41.2, 37.3, 35.1, 27.3, 20.1, 19.9. HRMS-ESI (m/z): [M + Na]$^+$ calcd for $C_{29}H_{38}N_2O_8SNa$ 597.2247, found 597.2251.

(3*S*,3a*R*,5*R*,6a*R*)-3-Hydroxyhexahydro-2*H*-cyclopenta[*b*]-furan-5-yl [(2*S*,3*R*)-3-Hydroxy-4-(*N*-isobutyl-4-methoxyphenylsulfonamido)-1-phenylbutan-2-yl]carbamate (22). A solution of keto inhibitor **21** (10 mg, 17 μmol) in EtOH was cooled to −25 °C, and $NaBH_4$ (6 mg) was added at once. The solution was stirred for 30 min. Then saturated aqueous NH_4Cl solution was added. The aqueous phase was extracted with EtOAc (×4). The combined organic layer was dried, filtered, and evaporated under reduced pressure. The residue was purified by column chromatography on silica gel using hexanes/EtOAc (2:1, 1:1, then 1:2) as the eluent to afford the desired inhibitor **22** (8 mg, 80%) as a white solid. TLC, R_f = 0.39 (hexanes/EtOAc = 1:5); ^{1}H NMR ($CDCl_3$, 500 MHz) δ 7.70 (d, J = 8.8 Hz, 2H), 7.32–7.19 (m, 5H), 6.97 (d, J = 8.8 Hz, 2H), 5.07 (m, 1H), 4.89 (d, J = 7.2 Hz, 1H), 4.38 (t, J = 6.8 Hz, 1H), 4.21 (m, 1H), 3.87 (s, 3H), 3.88–3.74 (m, 4H), 3.54 (dd, J = 3.2, 9.6 Hz, 1H), 3.10 (dd, J = 7.8, 15.0 Hz, 1H), 3.05–2.82 (m, 5H), 2.78 (dd, J = 6.8, 13.4 Hz, 1H), 2.42 (br s, 1H), 2.18–2.04 (m, 2H), 1.94–1.76 (m, 3H), 0.90 (d, J = 6.6 Hz, 3H), 0.86 (d, J = 6.6 Hz, 3H); ^{13}C NMR ($CDCl_3$, 125 MHz) δ 163.0, 155.3, 137.6, 129.9, 129.6, 129.5, 128.6, 126.5, 114.3, 84.9, 78.1, 76.3, 73.0, 72.2, 58.7, 55.6, 55.3, 53.7, 47.3, 39.1, 35.4, 31.3, 27.2, 20.1, 19.9; LRMS-ESI (m/z): [M + Na]$^+$ 599.3.

(3*S*,3a*R*,5*R*,6a*R*)-3-Hydroxyhexahydro-2*H*-cyclopenta[*b*]-furan-5-yl [(2*S*,3*R*)-4-(4-Amino-*N*-isobutylphenylsulfonamido)-3-hydroxy-1-phenylbutan-2-yl]carbamate (23). The ketone intermediate was first synthesized from the coupling of **19a** with isostere **20b** as described for **21** after stirring 48 h at room temperature in a CH_2Cl_2/THF (1:1) mixture. Purification of the crude compound by column chromatography on silica gel using chloroform with 1–3% EtOH as the eluent afforded the corresponding ketone inhibitor (60%, white solid). TLC, R_f = 0.18 (chloroform/3% EtOH); ^{1}H NMR ($CDCl_3$, 500 MHz) δ 7.54 (d, J = 8.6 Hz, 2H), 7.34–7.28 (m, 2H), 7.25–7.18 (m, 3H), 6.68 (d, J = 8.6 Hz, 2H), 5.02 (t, J = 6.9 Hz, 1H), 4.99 (m, 1H), 4.68 (d, J = 8.8 Hz, 1H), 4.14 (br s, 2H), 3.98 (s, 2H), 3.91 (m, 1H), 3.84–3.72 (m, 2H), 3.08 (dd, J = 8.4, 15.1 Hz, 1H), 3.00–2.83 (m, 5H), 2.76 (dd, J = 8.7, 13.4 Hz, 1H), 2.22–2.15 (m, 2H), 2.05–1.97 (m, 2H), 1.80 (m, 1H), 0.90 (d, J = 6.6 Hz, 3H), 0.86 (d, J = 6.6 Hz, 3H); ^{13}C NMR ($CDCl_3$, 125 MHz) δ 216.9, 155.4, 150.6, 137.5, 129.6, 129.5, 128.5, 126.5, 126.3, 114.1, 82.9, 76.3, 72.2, 70.6, 58.9, 55.0, 53.8, 48.7, 41.2, 37.3, 35.2, 27.3, 20.2, 19.9. HRMS-ESI (m/z): [M + Na$^+$] calcd for $C_{28}H_{37}N_3O_7SNa$ 582.2250, found 582.2246. The title compound was obtained in 82% yield by reduction of the above ketone intermediate as described for **22**, followed by column chromatography on silica gel using hexanes/EtOAc (1:2 to 1:5) as the eluent. Off-white solid. TLC, R_f = 0.12 (hexanes/EtOAc = 1:2); ^{1}H NMR ($CDCl_3$, 500 MHz) δ 7.54 (d, J = 8.8 Hz, 2H), 7.34–7.18 (m, 5H), 6.68 (d, J = 8.8 Hz, 2H), 5.07 (m, 1H), 4.87 (d, J = 7.2 Hz, 1H), 4.38 (t, J = 6.8 Hz, 1H), 4.24–4.19 (m, 1H), 4.14 (s, 2H), 3.86 (br s, 1H), 3.85–3.75 (m, 3H), 3.55 (dd, J = 3.6, 9.6 Hz, 1H), 3.10 (dd, J = 8.2, 15.0 Hz, 1H), 3.04–2.79 (m, 5H), 2.76 (dd, J = 6.8, 13.2 Hz, 1H), 2.37 (d, J = 11.6 Hz, 1H), 2.10 (t, J = 14.4 Hz, 2H), 1.94–1.75 (m, 3H), 0.90 (d, J = 6.8 Hz, 3H), 0.86 (d, J = 6.4 Hz, 3H); ^{13}C NMR ($CDCl_3$, 125 MHz) δ 155.3, 150.6, 137.6, 129.6, 129.5, 128.5, 126.5, 126.4, 114.1, 84.9, 78.0, 70.3, 73.0, 72.2, 58.8, 55.2, 53.7, 47.3, 39.1, 35.5, 31.3, 27.3, 20.2, 19.9. HRMS-ESI (m/z): [M + Na]$^+$ calcd for $C_{28}H_{39}N_3O_7SNa$ 584.2406, found 584.2410.

(3*S*,3a*R*,5*R*,6a*R*)-3-Hydroxyhexahydro-2*H*-cyclopenta[*b*]-furan-5-yl {(2*S*,3*R*)-3-Hydroxy-4-[4-(hydroxymethyl)-*N*-isobutylphenylsulfonamido]-1-phenylbutan-2-yl}carbamate (24). The ketone intermediate was first synthesized from the coupling of **19a** with isostere **20c** as described for **21**. Purification of the crude compound by column chromatography on silica gel using hexanes/EtOAc (2:1 to 1:2) as the eluent afforded the corresponding ketone inhibitor in 49% yield as a white solid. TLC, R_f = 0.38 (hexanes/EtOAc = 1:3); ^{1}H NMR ($CDCl_3$, 500 MHz) δ 7.76 (d, J = 8.2 Hz, 2H), 7.51 (d, J = 8.2 Hz, 2H), 7.34–7.28 (m, 2H), 7.25–7.20 (m, 3H), 5.02 (t, J = 6.9 Hz, 1H), 4.96 (m, 1H), 4.79 (s, 2H), 4.67 (d, J = 8.4 Hz, 1H), 3.98–3.93 (m, 2H), 3.84–3.75 (m, 2H), 3.75–3.67 (m, 1H), 3.10 (dd, J = 8.2, 15.1 Hz, 1H), 3.07–2.80 (m, 5H), 2.83 (dd, J = 6.9, 13.5 Hz, 1H), 2.23–2.15 (m, 2H), 2.04–1.96 (m, 2H), 1.88–1.76 (m, 1H), 0.90 (dd, J = 6.6 Hz, 3H), 0.87 (d, J = 6.6 Hz, 3H). The title compound was obtained in 83% yield by reduction of the above ketone intermediate as described for **22**, followed by column chromatography on silica gel using hexanes/EtOAc (1:1 to 1:3 and then 100% EtOAc) as the eluent. White solid. TLC, R_f = 0.23 (hexanes/EtOAc = 1:3); ^{1}H NMR ($CDCl_3$, 400 MHz) δ 7.76 (d, J = 8.2 Hz, 2H), 7.51 (d, J = 8.2 Hz, 2H), 7.34–7.27 (m, 2H), 7.24–7.20 (m, 3H), 5.06 (m, 1H), 4.82 (d, J = 7.8 Hz, 1H), 4.76 (s, 2H), 4.38 (t, J = 7.0 Hz, 1H), 4.21 (m, 1H), 3.85–3.68 (m, 4H), 3.55 (dd, J = 3.5, 9.8 Hz, 1H), 3.11 (dd, J = 8.3, 15.1 Hz, 1H), 3.05–2.79 (m, 6H), 2.38 (d, J = 8.3 Hz, 1H), 2.15–1.99 (m, 2H), 1.94–1.80 (m, 3H), 0.91 (d, J = 6.6 Hz, 3H), 0.87 (d, J = 6.6 Hz, 3H). HRMS-ESI (m/z): [M + Na]$^+$ calcd for $C_{29}H_{40}N_2O_8SNa$ 599.2403, found 599.2401.

(3*S*,3a*S*,5*R*,6a*R*)-3-Methoxyhexahydro-2*H*-cyclopenta[*b*]-furan-5-yl [(2*S*,3*R*)-3-Hydroxy-4-(*N*-isobutyl-4-methoxyphenylsulfonamido)-1-phenylbutan-2-yl]carbamate (25). The title compound was obtained in 73% yield from **19b** and **20a** as described for **21** following column chromatography on silica gel using hexanes/EtOAc (1:1) as the eluent. White solid. TLC, R_f = 0.21 (hexanes/EtOAc = 1:1); ^{1}H NMR ($CDCl_3$, 500 MHz) δ 7.70 (d, J = 8.9 Hz, 2H), 7.33–7.19 (m, 5H), 6.97 (d, J = 8.9 Hz, 2H), 4.97–4.90 (m, 1H), 4.78 (d, J = 7.5 Hz, 1H), 4.47–4.42 (m, 1H), 3.99 (q, J = 6.9 Hz, 1H), 3.87 (s, 3H), 3.88–3.82 (m, 2H), 3.81–3.76 (m, 2H), 3.70 (dd, J = 6.9, 9.0 Hz, 1H), 3.30 (s, 3H), 3.14–3.06 (dd, J = 7.8, 14.9 Hz, 1H), 3.04–2.88 (m, 4H), 2.78 (dd, J = 6.7, 13.4 Hz, 1H), 2.70 (m, 1H), 2.14 (m, 1H), 1.93 (dd, J = 6.3, 8.6 Hz, 2H), 1.86–1.76 (m, 2H), 0.90 (d, J = 6.6 Hz, 3H), 0.86 (d, J = 6.6 Hz, 3H); ^{13}C NMR ($CDCl_3$, 125 MHz) δ 163.0, 156.3, 137.5, 129.9, 129.6, 129.5, 128.5, 126.5, 114.3, 83.5, 81.3, 76.3, 72.3, 70.0, 58.7, 57.8, 55.6, 54.9, 53.7, 43.8, 39.5, 35.5, 30.4, 27.2, 20.1, 19.9. HRMS-ESI (m/z): [M + H] $^+$ calcd for $C_{30}H_{43}N_2O_8S$ 591.2740, found 591.2742.

(3*R*,3a*R*,5*R*,6a*R*)-3-Hydroxyhexahydro-2*H*-cyclopenta[*b*]-furan-5-yl [(2*S*,3*R*)-3-Hydroxy-4-(*N*-isobutyl-4-methoxyphenylsulfonamido)-1-phenylbutan-2-yl]carbamate (26). The

acetyl intermediate was first synthesized in 84% yield by coupling of **19c** with **20a** as described for **21** followed by purification by column chromatography on silica gel using hexanes/EtOAc (3:1 to 1:1) as the eluent. White solid. TLC, R_f = 0.23 (hexanes/EtOAc = 1:2); ^{1}H NMR ($CDCl_3$, 300 MHz) δ 7.71 (d, J = 8.9 Hz, 2H), 7.34−7.19 (m, 5H), 6.97 (d, J = 8.9 Hz, 2H), 4.91 (m, 1H), 4.88 (m, 1H), 4.75 (d, J = 8.2 Hz, 1H), 4.67 (m, 1H), 3.98 (dd, J = 4.1, 10.4 Hz, 1H), 3.87 (s, 3H), 3.85−3.77 (m, 3H), 3.73 (dd, J = 1.5, 10.4 Hz, 1H), 3.19−2.92 (m, 4H), 2.90−2.72 (m, 2H), 2.67−2.55 (m, 1H), 2.23−2.09 (m, 1H), 2.06 (s, 3H), 2.04−1.76 (m, 3H), 1.50−1.43 (m, 1H), 0.91 (d, J = 6.6 Hz, 3H), 0.87 (d, J = 6.6 Hz, 3H); ^{13}C NMR ($CDCl_3$, 75 MHz) δ 170.6, 163.0, 156.0, 137.6, 129.8, 129.5, 128.5, 126.6, 114.3, 83.5, 80.6, 76.1, 72.6, 71.6, 58.8, 55.6, 54.9, 53.7, 48.5, 39.6, 36.2, 35.7, 27.2, 21.1, 20.1, 19.9. The acetate intermediate (18 mg, 0.029 mmol) was diluted in MeOH (1.5 mL) at 0 °C. K_2CO_3 (5 mg, 0.04 mmol) was added, and the solution was stirred for 6 h. Saturated aqueous NH_4Cl solution (1 mL) was added, and the solvent was reduced under vacuum. The aqueous phase was diluted and extracted with EtOAc (×4). The combined organic phase was dried ($MgSO_4$), filtered, and evaporated. The residue was purified by column chromatography on silica gel using (chloroform)/(0.5−3% EtOH) as the eluent to provide inhibitor **26** (15.9 mg, 94%) as a white solid. TLC, R_f = 0.26 (hexanes/EtOAc = 1:5); ^{1}H NMR ($CDCl_3$, 500 MHz) δ 7.71 (d, J = 8.9 Hz, 2H), 7.33−7.25 (m, 1H), 7.24−7.19 (m, 3H), 6.98 (d, J = 8.9 Hz, 2H), 4.86 (m, 1H), 4.81 (d, J = 8.3 Hz, 1H), 4.69 (t, J = 5.4 Hz, 1H), 4.01 (m, 1H), 3.91−3.76 (m, 4H), 3.87 (s, 3H), 3.64 (dd, J = 2.0, 9.7 Hz, 1H), 3.12 (dd, J = 8.2, 15.1 Hz, 1H), 3.11−3.05 (m, 1H), 3.03 (dd, J = 2.7, 15.2 Hz, 1H), 2.95 (dd, J = 8.3, 13.4 Hz, 1H), 2.85−2.75 (m, 2H), 2.52 (m, 1H), 2.12 (ddd, J = 6.1, 10.0, 14.7 Hz, 1H), 1.99 (dt, J = 6.1, 15.0 Hz, 1H), 1.93−1.79 (m, 3H), 1.35 (m, 1H), 0.91 (d, J = 6.6 Hz, 3H), 0.87 (d, J = 6.6 Hz, 3H); ^{13}C NMR ($CDCl_3$, 125 MHz) δ 163.0, 156.0, 137.8, 129.8, 129.5, 128.4, 126.4, 114.3, 83.1, 78.3, 76.3, 73.8, 72.7, 58.8, 55.6, 54.8, 53.7, 51.3, 39.5, 36.1, 35.8, 27.2, 20.1, 19.9. HRMS-ESI (m/z): $[M + H]^+$ calcd for $C_{29}H_{41}N_2O_8S$ 577.2584, found 577.2572.

(3*R*,3a*R*,5*R*,6a*R*)-3-Hydroxyhexahydro-2*H*-cyclopenta[*b*]-furan-5-yl [(2*S*,3*R*)-4-(4-Amino-*N*-isobutylphenylsulfonamido)-3-hydroxy-1-phenylbutan-2-yl]carbamate (27). The acetyl intermediate was first synthesized in 63% yield by coupling of **19c** with **20b** as described for **21** followed by purification by column chromatography on silica gel using ($CHCl_3$)/(0.25−1.5% EtOH) as the eluent. White solid. TLC, R_f = 0.44 (hexanes/EtOAc = 1:3); ^{1}H NMR ($CDCl_3$, 500 MHz) δ 7.54 (d, J = 8.7 Hz, 2H), 7.32−7.27 (m, 2H), 7.25−7.19 (m, 3H), 6.67 (d, J = 8.7 Hz, 2H), 4.94 (m, 1H), 4.90−4.85 (m, 1H), 4.75 (d, J = 8.7 Hz, 1H), 4.66 (t, J = 5.4 Hz, 1H), 4.16 (br s, 2H), 3.99 (dd, J = 4.1, 10.4 Hz, 1H), 3.88−3.77 (m, 3H), 3.74 (d, J = 10.3 Hz, 1H), 3.11 (dd, J = 8.5, 15.1 Hz, 1H), 3.05 (dd, J = 4.0, 14.1 Hz, 1H), 2.98 (dd, J = 1.5, 15.2 Hz, 1H), 2.93 (dd, J = 8.4, 13.2 Hz, 1H), 2.84 (dd, J = 8.8, 13.9 Hz, 1H), 2.77 (dd, J = 6.7, 13.3 Hz, 1H), 2.64−2.56 (m, 1H), 2.20−2.12 (m, 1H), 2.07 (s, 3H), 2.00 (dt, J = 6.1, 15.2 Hz, 1H), 1.95−1.88 (m, 1H), 1.81 (m, 1H), 1.51−1.44 (m, 1H), 0.91 (d, J = 6.6 Hz, 3H), 0.87 (d, J = 6.6 Hz, 3H); ^{13}C NMR ($CDCl_3$, 125 MHz) δ 170.6, 155.9, 150.6, 137.7, 129.5, 128.5, 126.5, 126.2, 114.1, 83.5, 80.6, 76.0, 72.6, 71.5, 58.9, 54.9, 53.8, 48.5, 39.6, 36.2, 35.7, 27.3, 21.1, 20.2, 19.9. The title compound was obtained from the above acetate intermediate in 88% yield as described for **26** following purification by column chromatography on silica gel using a gradient, 1−5% EtOH in $CHCl_3$, as the eluent. White solid. TLC, R_f = 0.4 ($CHCl_3$/10% EtOH); ^{1}H NMR ($CDCl_3$, 500 MHz) δ 7.55 (d, J = 8.7 Hz, 2H), 7.31−7.26 (m, 2H), 7.24−7.19 (m, 3H), 6.67 (d, J = 8.7 Hz, 2H), 4.89−4.83 (m, 1H), 4.79 (d, J = 8.9 Hz, 1H), 4.69 (t, J = 5.4 Hz, 1H), 4.16 (br s, 2H), 4.01 (m, 1H), 3.88 (dd, J = 3.7, 9.9 Hz, 1H), 3.87−3.76 (m, 3H), 3.65 (dd, J = 1.4, 9.8 Hz, 1H), 3.14−3.04 (m, 2H), 2.99 (dd, J = 2.9, 15.1 Hz, 1H), 2.92 (dd, J = 8.3, 13.3 Hz, 1H), 2.81 (dd, J = 9.1, 14.0 Hz, 1H), 2.78 (dd, J = 6.8, 13.3 Hz, 1H), 2.54−2.47 (m, 1H), 2.11 (ddd, J = 6.2, 10.2, 14.6 Hz, 1H), 2.00 (dt, J = 6.1, 15.1 Hz, 1H), 1.93−1.85 (m, 1H), 1.85−1.76 (m, 2H), 1.35 (m, 1H), 0.91 (d, J = 6.6 Hz, 3H), 0.87 (d, J = 6.6 Hz, 3H); ^{13}C NMR ($CDCl_3$, 125 MHz) δ 156.0, 150.7, 137.8, 129.5, 128.4, 126.4, 126.2, 114.1, 83.1, 78.3, 76.2, 73.7, 72.7, 58.9, 54.8, 53.8, 51.3, 39.5, 36.0, 35.8, 27.3, 20.2, 19.9. HRMS-ESI (m/z): $[M + H]^+$ calcd for $C_{28}H_{39}N_3O_7S$ 584.2406, found 584.2398.

(3*R*,3a*S*,5*R*,6a*R*)-3-Methoxyhexahydro-2*H*-cyclopenta[*b*]-furan-5-yl [(2*S*,3*R*)-3-Hydroxy-4-(*N*-isobutyl-4-methoxyphenylsulfonamido)-1-phenylbutan-2-yl]carbamate (28). The title compound was obtained in 57% yield from **19d** and **20a** as described for **21** following purification by column chromatography on silica gel using hexanes/EtOAc (2:1 to 1:1) as the eluent. White solid. TLC, R_f = 0.34 (hexanes/EtOAc = 1:2); ^{1}H NMR ($CDCl_3$, 500 MHz) δ 7.71 (d, J = 8.8 Hz, 2H), 7.33−7.25 (m, 2H), 7.26−7.20 (m, 3H), 6.98 (d, J = 8.8 Hz, 2H), 4.89 (m, 1H), 4.78 (d, J = 8.3 Hz, 1H), 4.61 (t, J = 5.7 Hz, 1H), 3.93−3.85 (m, 1H), 3.88 (s, 3H), 3.85−3.79 (m, 2H), 3.73 (d, J = 2.7, 9.8 Hz, 1H), 3.60 (m, 1H), 3.31 (s, 3H), 3.13 (dd, J = 8.3, 15.2 Hz, 1H), 3.10−3.00 (m, 2H), 2.95 (dd, J = 8.4, 13.4 Hz, 1H), 2.88−2.77 (m, 1H), 2.80 (dd, J = 7.0, 13.3 Hz, 1H), 2.62−2.53 (m, 1H), 2.19−2.09 (m, 1H), 1.99 (dt, J = 6.0, 15.1 Hz, 1H), 1.92 (m, 1H), 1.90−1.78 (m, 2H), 1.47−1.38 (m, 1H), 0.92 (d, J = 6.6 Hz, 3H), 0.88 (d, J = 6.6 Hz, 3H); ^{13}C NMR ($CDCl_3$, 125 MHz) δ 163.0, 156.1, 137.7, 129.9, 129.5, 128.5, 126.5, 114.3, 87.6, 83.3, 76.5, 72.7, 71.1, 58.8, 56.7, 55.6, 54.9, 53.7, 48.0, 39.5, 36.6, 35.8, 27.2, 20.1, 19.9. HRMS-ESI (m/z): $[M + Na]^+$ calcd for $C_{30}H_{42}N_2O_8SNa$ 613.2560, found 613.2555.

(3*S*,3a*R*,5*R*,6a*R*)-3-Methylhexahydro-2*H*-cyclopenta[*b*]-furan-5-yl [(2*S*,3*R*)-3-Hydroxy-4-(*N*-isobutyl-4-methoxyphenylsulfonamido)-1-phenylbutan-2-yl]carbamate (29). The title compound was obtained from **19e** and **20a** in 78% yield as described for **21** following purification by column chromatography on silica gel using hexanes/EtOAc (3:1 to 2:1) as the eluent. White solid. TLC, R_f = 0.32 (hexanes/EtOAc = 1:1); ^{1}H NMR ($CDCl_3$, 300 MHz) δ 7.71 (d, J = 8.9 Hz, 2H), 7.34−7.19 (m, 5H), 6.98 (d, J = 8.9 Hz, 2H), 4.84 (m, 1H), 4.75 (d, J = 8.2 Hz, 1H), 4.49−4.40 (m, 1H), 3.87 (s, 3H), 3.86−3.76 (m, 4H), 3.32 (dd, J = 8.3, 10.5 Hz, 1H), 3.11 (dd, J = 7.8, 15.1 Hz, 1H), 3.06−2.84 (m, 4H), 2.79 (dd, J = 6.7, 13.4 Hz, 1H), 2.54−2.45 (m, 1H), 2.40−2.31 (m, 1H), 2.18 (dt, J = 6.5, 14.8 Hz, 1H), 1.90−1.77 (m, 2H), 1.74−1.66 (m, 1H), 1.50−1.40 (m, 1H), 0.91 (d, J = 6.8 Hz, 3H), 0.90 (d, J = 6.6 Hz, 3H), 0.86 (d, J = 6.6 Hz, 3H); ^{13}C NMR ($CDCl_3$, 75 MHz) δ 162.7, 156.3, 137.6, 129.8, 129.5, 128.5, 126.5, 114.3, 83.5, 76.0, 72.6, 72.2, 58.7, 55.6, 54.9, 53.7, 45.6, 39.8, 36.4, 35.6, 31.3, 27.2, 20.1, 19.8, 11.8. LRMS-ESI (m/z): $[M + Na]^+$ 597.3, $[M + H]^+$ 575.1.

(3*R*,3a*R*,5*R*,6a*R*)-3-Methylhexahydro-2*H*-cyclopenta[*b*]-furan-5-yl [(2*S*,3*R*)-3-Hydroxy-4-(*N*-isobutyl-4-methoxyphenylsulfonamido)-1-phenylbutan-2-yl]carbamate (30). The title compound was obtained from **19f** and **20a** in 96% yield as described for **21** following purification by column chromatography on silica gel using hexanes/EtOAc (5:1) as the eluent. White solid. TLC, R_f = 0.50 (hexanes/EtOAc = 1:1); $[\alpha]_D^{20}$ +24.5 (c 1.0, $CHCl_3$); ^{1}H NMR ($CDCl_3$, 400 MHz) δ 7.70 (d, J = 8.8 Hz, 2H), 7.30−7.16 (m, 5H), 6.96 (d, J = 8.8 Hz, 2H), 4.88 (m, 1H), 4.80 (d, J = 7.1 Hz, 1H), 4.46 (m, 1H), 3.91 (dd, J = 6.1, 8.5 Hz, 1H), 3.86 (s, 3H), 3.80 (m, 3H), 3.22 (dd, J = 7.5, 14.8 Hz, 1H), 3.15−2.99 (m, 3H), 2.94 (dd, J = 8.2, 13.4 Hz, 1H), 2.87−2.75 (m, 2H), 2.14 (m, 1H), 2.00−1.77 (m, 5H), 1.50 (d, J = 12.3 Hz, 1H), 0.98 (d, J = 6.6 Hz, 3H), 0.90 (d, J = 6.6 Hz, 3H), 0.85 (d, J = 6.6 Hz, 3H); ^{13}C NMR ($CDCl_3$, 100 MHz) δ 162.9, 156.2, 137.7, 129.8, 129.4, 128.4, 126.4, 114.3, 83.7, 77.2, 74.7, 72.5, 58.7, 55.6, 54.8, 53.7, 50.2, 41.8, 39.4, 37.7, 35.7, 27.2, 20.1, 19.8, 17.6. LRMS-ESI (m/z): $[M + Na]^+$ 597.1, $[M + H]^+$ 575.3.

(3*S*,3a*R*,5*R*,6a*R*)-3-(Dimethylamino)hexahydro-2*H*-cyclopenta[*b*]furan-5-yl [(2*S*,3*R*)-3-Hydroxy-4-(*N*-isobutyl-4-methoxyphenylsulfonamido)-1-phenylbutan-2-yl]carbamate (31). To a solution of AcOH (~15 μL) in dichloromethane (1 mL), a slow

stream of Me_2NH gas was bubbled briefly at 0 °C for 5 min. After the flask was flushed with argon, a solution of ketone inhibitor **21** (13 mg, 0.02 mmol) in dichloroethane (0.5 mL) was added at 0 °C, and after 15 min, $NaBH(OAc)_3$ (10 mg, 0.05 mmol) was added. The resulting solution was warmed to room temperature. After 24 h, another 10 mg portion of $NaBH(OAc)_3$ was added and the solution stirred for 48 h. The reaction was quenched by addition of saturated aqueous $NaHCO_3$ solution, adjusting the pH to 10 with 1 M NaOH solution. The aqueous phase was extracted multiple times with EtOAc. The combined organic phase was dried (Na_2SO_4), filtered, and evaporated under reduced pressure. The residue was purified by column chromatography on silica gel using ethanol (0.5−2%) in $CHCl_3$ to furnish the corresponding dimethylamine inhibitor **31** (11.3 mg, 82%) as a white solid. TLC, R_f = 0.35 ($CHCl_3$/8% EtOH); ^1H NMR ($CDCl_3$, 500 MHz) δ 7.70 (d, J = 8.9 Hz, 2H), 7.32−7.26 (m, 2H), 7.25−7.19 (m, 3H), 6.97 (d, J = 8.9 Hz, 2H), 4.92 (m, 1H), 4.86 (m, 1H), 4.55 (m, 1H), 3.90−3.85 (m, 1H), 3.87 (s, 3H), 3.83−3.75 (m, 2H) 3.70−3.63 (m, 1H), 3.30−3.20 (m, 1H), 3.10 (dd, J = 3.14, 3.06 Hz, 1H), 3.04−2.88 (m, 4H), 2.79 (dd, J = 6.9, 13.4 Hz, 1H), 2.64−2.55 (m, 1H), 2.23−2.18 (m, 1H), 2.24 (br s, 6H), 2.18−2.10 (m, 1H), 2.06−1.97 (m, 1H), 1.88−1.75 (m, 2H), 0.90 (d, J = 6.6 Hz, 3H), 0.85 (d, J = 6.6 Hz, 3H); ^{13}C NMR ($CDCl_3$, 125 MHz) δ 163.0, 156.4, 137.6, 130.0, 129.6, 129.5, 128.5, 126.5, 114.3, 83.8, 77.2, 76.0, 72.3, 69.4, 58.7, 55.6, 55.0, 53.7, 45.4, 45.3, 40.1, 35.5, 31.4, 27.2, 20.1, 19.9. LRMS-ESI (m/z): $[M + H]^+$ 604.3

Determination of X-ray Structure of HIV-1 Protease Inhibitor Complex. The optimized HIV-1 protease was expressed and purified as previously described.[23] The protease−inhibitor complex was crystallized by the hanging drop vapor diffusion method with well solutions of 1.2 M ammonium chloride and 0.1 M sodium acetate buffer (pH 4.8). Diffraction data were collected on a single crystal cooled to 90 K at SER-CAT BM beamline 22, Advanced Photon Source, Argonne National Laboratory (Chicago, IL, U.S.), with an X-ray wavelength of 1.0 Å and processed by HKL-2000[24] with R_{merge} of 7.2%. The PR structure was used in molecular replacement by PHASER[25,26] in the CCP4i suite[27,28] and refined to 1.45 Å resolution using SHELX-97[29,30] and COOT[31] for manual modification. PRODRG-2[32] was used to construct the inhibitor and the restraints for refinement. Alternative conformations were modeled, anisotropic atomic displacement parameters (B factors) were applied for all atoms including solvent molecules, and hydrogen atoms were added in the final round of refinement. The final refined solvent structure comprised two Cl^- ions and 142 water molecules. The crystallographic statistics are listed in Table 3 in the Supporting Information. The coordinates and structure factors of the PR with **26** complex have been deposited in Protein Data Bank[33] with code 3ST5.

■ ASSOCIATED CONTENT

Supporting Information. HPLC, LRMS, and HRMS data of inhibitors **21**−**31**; crystallographic data collection and refinement statistics for inhibitor **26**. This material is available free of charge via the Internet at http://pubs.acs.org.

Accession Codes

†The PDB accession code for **26**-bound HIV-1 protease X-ray structure is 3ST5.

■ AUTHOR INFORMATION

Corresponding Author

*Phone: (765) 494-5323. Fax: (765) 496-1612. E-mail: akghosh@purdue.edu.

■ ACKNOWLEDGMENT

This research was supported by the National Institutes of Health (Grant GM53386 to A.K.G. and Grant GM62920 to I.T. W.). This work was also supported by the Intramural Research Program of the Center for Cancer Research, National Cancer Institute, National Institutes of Health, and in part by a Grant-in-Aid for Scientific Research (Priority Areas) from the Ministry of Education, Culture, Sports, Science, and Technology of Japan (Monbu Kagakusho), a Grant for Promotion of AIDS Research from the Ministry of Health, Welfare, and Labor of Japan, and the Grant to the Cooperative Research Project on Clinical and Epidemiological Studies of Emerging and Reemerging Infectious Diseases (Renkei Jigyo) of Monbu-Kagakusho.

■ ABBREVIATIONS USED

bis-THF, bis-tetrahydrofuran; Cp-THF, hexahydrocyclopentafuran; PI, protease inhibitor; APV, amprenavir; DRV, darunavir; SQV, saquinavir; IDV, indinavir; TBS, *tert*-butyldimethylsilyl; DIBAL, diisobutylaluminum hydride

■ REFERENCES

(1) Palella, F. J., Jr.; Delaney, K. M.; Moorman, A. C.; Loveless, M. O.; Fuhrer, J.; Satten, G. A.; Aschman, D. J.; Holmberg, S. D. Declining Morbidity and Mortality among Patients with Advanced Human Immunodeficiency Virus Infection. *N. Engl. J. Med.* **1998**, *338*, 853–860.

(2) Sepkowitz, K. A. AIDS—The First 20 Years. *N. Engl. J. Med.* **2001**, *344*, 1764–1772.

(3) Gupta, R.; Hill, A.; Sawyer, A. W.; Pillay, D. Emergence of Drug Resistance in HIV Type 1-Infected Patients after Receipt of First-Line Highly Active Antiretroviral Therapy: A Systematic Review of Clinical Trials. *Clin. Infect. Dis.* **2008**, *47*, 712–722.

(4) Wainberg, M. A.; Friedland, G. Public Health Implications of Antiretroviral Therapy and HIV Drug Resistance. *JAMA, J. Am. Med. Assoc.* **1998**, *279*, 1977–1983.

(5) Ghosh, A. K.; Chapsal, B. D.; Weber, I. T.; Mitsuya, H. Design of HIV Protease Inhibitors Targeting Protein Backbone: An Effective Strategy for Combating Drug Resistance. *Acc. Chem. Res.* **2008**, *41*, 78–86.

(6) Ghosh, A. K.; Sridhar, P. R.; Kumaragurubaran, N.; Koh, Y.; Weber, I. T.; Mitsuya, H. Bis-Tetrahydrofuran: A Privileged Ligand for Darunavir and a New Generation of HIV Protease Inhibitors That Combat Drug Resistance. *ChemMedChem.* **2006**, *1*, 939–950.

(7) Koh, Y.; Nakata, H.; Maeda, K.; Ogata, H.; Bilcer, G.; Devasamudram, T.; Kincaid, J. F.; Boross, P.; Wang, Y.-F.; Tie, Y.; Volarath, P.; Gaddis, L.; Harrison, R. W.; Weber, I. T.; Ghosh, A. K.; Mitsuya, H. Novel Bis-tetrahydrofuranylurethane-Containing Nonpeptidic Protease Inhibitor (PI) UIC-94017 (TMC114) with Potent Activity against Multi-PI-Resistant Human Immunodeficiency Virus in Vitro. *Antimicrob. Agents Chemother.* **2003**, *47*, 3123–3129.

(8) Ghosh, A.; Chapsal, B.; Mitsuya, H. In *Aspartic Acid Proteases as Therapeutic Targets*; Ghosh, A., Ed.; Wiley-VCH Verlag GmbH & Co. KGaA: Weinheim, Germany, 2010; pp 245−262.

(9) Ghosh, A. K.; Dawson, Z. L.; Mitsuya, H. Darunavir, a Conceptually New HIV-1 Protease Inhibitor for the Treatment of Drug-Resistant HIV. *Bioorg. Med. Chem. Lett.* **2007**, *15*, 7576–7580.

(10) Ghosh, A. K.; Sridhar, P. R.; Leshchenko, S.; Hussain, A. K.; Li, J.; Kovalevsky, A. Y.; Walters, D. E.; Wedekind, J. E.; Grum-Tokars, V.; Das, D.; Koh, Y.; Maeda, K.; Gatanaga, H.; Weber, I. T.; Mitsuya, H. Structure-Based Design of Novel HIV-1 Protease Inhibitors To Combat Drug Resistance. *J. Med. Chem.* **2006**, *49*, 5252–5261.

(11) Ghosh, A. K.; Leshchenko-Yashchuk, S.; Anderson, D. D.; Baldridge, A.; Noetzel, M.; Miller, H. B.; Tie, Y. F.; Wang, Y.-F.; Koh, Y.; Weber, I. T.; Mitsuya, H. Design of HIV-1 Protease Inhibitors with

Pyrrolidinones and Oxazolidinones as Novel P1′-Ligands To Enhance Backbone-Binding Interactions with Protease: Synthesis, Biological Evaluation, and Protein−Ligand X-ray Studies. *J. Med. Chem.* **2009**, *52*, 3902–3914.

(12) Koh, Y.; Das, D.; Leschenko, S.; Nakata, H.; Ogata-Aoki, H.; Amano, M.; Nakayama, M.; Ghosh, A. K.; Mitsuya, H. GRL-02031, a Novel Nonpeptidic Protease Inhibitor (PI) Containing a Stereochemically Defined Fused Cyclopentanyltetrahydrofuran Potent against Multi-PI-Resistant Human Immunodeficiency Virus Type 1 in Vitro. *Antimicrob. Agents Chemother.* **2009**, *53*, 997–1006.

(13) Deardorff, D. R.; Windham, C. Q.; Craney, C. L. *Org. Synth., Collect. Vol.* **1998**, *9*, 487.

(14) Ghosh, A. K.; Chapsal, B. D.; Baldridge, A.; Ide, K.; Koh, Y.; Mitsuya, H. Design and Synthesis of Stereochemically Defined Novel Spirocyclic P2-Ligands for HIV-1 Protease Inhibitors. *Org. Lett.* **2008**, *10*, 5135–5138.

(15) Hays, D. S.; Fu, G. C. Organotin Hydride Catalyzed Carbon−Carbon Bond Formation: Radical-Mediated Reductive Cyclization of Enals and Enones. *J. Org. Chem.* **1996**, *61*, 4–5.

(16) Bueno, J. M.; Coterón, J. M.; Chiara, J. L.; Fernández-Mayoralas, A.; Fiandor, J. M.; Valle, N. Stereoselective Synthesis of the Antifungal GM222712. *Tetrahedron Lett.* **2000**, *41*, 4379–4382.

(17) Ghosh, A. K.; Chapsal, B. D.; Baldridge, A.; Steffey, M. P.; Walters, D. E.; Koh, Y.; Amano, M.; Mitsuya, H. Design and Synthesis of Potent HIV-1 Protease Inhibitors Incorporating Hexahydrofuropyranol-Derived High Affinity P2 Ligands: Structure −Activity Studies and Biological Evaluation. *J. Med. Chem.* **2011**, *54*, 622–634.

(18) Toth, M. V.; Marshall, G. R. A Simple Continuous Fluorometric Assay for HIV Protease. *Int. J. Pept. Protein Res.* **1990**, *36*, 544–550.

(19) Ghosh, A. K.; Kulkarni, S.; Anderson, D. D.; Hong, L.; Baldridge, A.; Wang, Y.-F.; Chumanevich, A. A.; Kovalevsky, A. Y.; Tojo, Y.; Amano, M.; Koh, Y.; Tang, J.; Weber, I. T.; Mitsuya, H. Design, Synthesis, Protein−Ligand X-ray Structure, and Biological Evaluation of a Series of Novel Macrocyclic Human Immunodeficiency Virus-1 Protease Inhibitors To Combat Drug Resistance. *J. Med. Chem.* **2009**, *52*, 7689–7705.

(20) Kovalevsky, A. Y.; Liu, F.; Leshchenko, S.; Ghosh, A. K.; Louis, J. M.; Harrison, R. W.; Weber, I. T. Ultra-High Resolution Crystal Structure of HIV-1 Protease Mutant Reveals Two Binding Sites for Clinical Inhibitor TMC114. *J. Mol. Biol.* **2006**, *363*, 161–173.

(21) Gustchina, A.; Sansom, C.; Prevost, M.; Richelle, J.; Wodak, S. Y.; Wlodawer, A.; Weber, I. T. Energy Calculations and Analysis of HIV-1 Protease−Inhibitor Crystal Structures. *Protein Eng.* **1994**, *7*, 309–316.

(22) Tie, Y.; Boross, P. I.; Wang, Y. F.; Gaddis, L.; Liu, F.; Chen, X.; Tozser, J.; Harrison, R. W.; Weber, I. T. Molecular Basis for Substrate Recognition and Drug Resistance from 1.1 to 1.6 Å Resolution Crystal Structures of HIV-1 Protease Mutants with Substrate Analogs. *FEBS J.* **2005**, *272*, 5265–5277.

(23) Mahalingam, B.; Louis, J. M.; Hung, J.; Harrison, R. W.; Weber, I. T. Structural Implications of Drug-Resistant Mutants of HIV-1 Protease: High Resolution Crystal Structures of the Mutant Protease/Substrate Analog Complexes. *Proteins* **2001**, *43*, 455–464.

(24) Otwinowski, Z.; Minor, W. Processing of X-ray Diffraction Data Collected in Oscillation Mode. *Macromolecular Crystallography, Part A*; Carter, C. W., Jr., Sweet, R. M., Eds.; Methods in Enzymology, Vol. 276; Academic Press: San Diego, CA, 1997; pp 307−326.

(25) Shen, C. H.; Wang, Y. F.; Kovalevasky, A. Y.; Harrison, R. W.; Weber, I. T. Amprenavir Complexes with HIV-1 Protease and Its Drug-Resistant Mutants Altering Hydrophobic Clusters. *FEBS J.* **2010**, *277* (18), 3699–3714.

(26) McCoy, A. J.; Grosse-Kunstleve, R. W.; Adams, P. D.; Winn, M. D.; Storoni, L. C.; Read, R. J. Phaser Crystallographic Software. *J. Appl. Crystallogr.* **2007**, *40*, 658–674.

(27) Collaborative Computational Project, Number 4. The CCP4 Suite: Programs for Protein Crystallography. *Acta Crystallogr., Sect. D: Biol. Crystallogr.*, **1994**, *50*, 760−763.

(28) Potterton, E.; Briggs, P.; Turkenburg, M.; Dodson, E. A Graphical User Interface to the CCP4 Program Suite. *Acta Crystallogr., Sect. D: Biol. Crystallogr.* **2003**, *59*, 1131–1137.

(29) Sheldrick, G. M. A Short History of SHELX. *Acta Crystallogr., Sect. A: Found. Crystallogr.* **2008**, *64*, 112–122.

(30) Sheldrick, G. M.; Schneider, T. R. SHELXL: High Resolution Refinement. *Methods Enzymol.* **1997**, *277*, 319–343.

(31) Emsley, P.; Cowtan, K. Coot: Model-Building Tools for Molecular Graphics. *Acta Crystallogr., Sect. D: Biol. Crystallogr.* **2004**, *60*, 2126–2132.

(32) Schuettelkopf, A. W.; van Aalten, D. M. F. PRODRG: A Tool for High-Throughput Crystallography of Protein−Ligand Complexes. *Acta Crystallogr., Sect. D: Biol. Crystallogr.* **2004**, *60*, 1355–1363.

(33) Berman, H. M.; Westbrook, J.; Feng, Z.; Gilliland, G.; Bhat, T. N.; Weissig, H.; Shindyalov, I. N.; Bourne, P. E. The Protein Data Bank. *Nucleic Acids Res.* **2000**, *28*, 235–242.

JOURNAL OF VIROLOGY, Oct. 2011, p. 10079–10089 Vol. 85, No. 19
0022-538X/11/$12.00 doi:10.1128/JVI.05121-11

Loss of Protease Dimerization Inhibition Activity of Darunavir Is Associated with the Acquisition of Resistance to Darunavir by HIV-1[▽]

Yasuhiro Koh,[1] Manabu Aoki,[1,2] Matthew L. Danish,[1] Hiromi Aoki-Ogata,[1] Masayuki Amano,[1] Debananda Das,[3] Robert W. Shafer,[4] Arun K. Ghosh,[5] and Hiroaki Mitsuya[1,3]*

Departments of Infectious Diseases and Hematology, Kumamoto University Graduate School of Medical Sciences, Kumamoto 860-8556, Japan[1]; Department of Medical Technology, Kumamoto Health Science University, Kumamoto 861-5598, Japan[2]; Experimental Retrovirology Section, HIV and AIDS Malignancy Branch, National Cancer Institute, National Institutes of Health, Bethesda, Maryland 20892[3]; Division of Infectious Diseases, Stanford University Medical Center, Stanford, California 94305[4]; and Departments of Chemistry and Medicinal Chemistry, Purdue University, West Lafayette, Indiana 47907[5]

Received 13 May 2011/Accepted 22 July 2011

Dimerization of HIV protease is essential for the acquisition of protease's proteolytic activity. We previously identified a group of HIV protease dimerization inhibitors, including darunavir (DRV). In the present work, we examine whether loss of DRV's protease dimerization inhibition activity is associated with HIV development of DRV resistance. Single amino acid substitutions, including I3A, L5A, R8A/Q, L24A, T26A, D29N, R87K, T96A, L97A, and F99A, disrupted protease dimerization, as examined using an intermolecular fluorescence resonance energy transfer (FRET)-based HIV expression assay. All recombinant HIV_{NL4-3}-based clones with such a protease dimerization-disrupting substitution failed to replicate. A highly DRV-resistant *in vitro*-selected HIV variant and clinical HIV strains isolated from AIDS patients failing to respond to DRV-containing antiviral regimens typically had the V32I, L33F, I54M, and I84V substitutions in common in protease. None of up to 3 of the 4 substitutions affected DRV's protease dimerization inhibition, which was significantly compromised by the four combined substitutions. Recombinant infectious clones containing up to 3 of the 4 substitutions remained sensitive to DRV, while a clonal HIV variant with all 4 substitutions proved highly resistant to DRV with a 205-fold 50% effective concentration (EC_{50}) difference compared to HIV_{NL4-3}. The present data suggest that the loss of DRV activity to inhibit protease dimerization represents a novel mechanism contributing to HIV resistance to DRV. The finding that 4 substitutions in PR are required for significant loss of DRV's protease dimerization inhibition should at least partially explain the reason DRV has a high genetic barrier against HIV's acquisition of DRV resistance.

Currently available combination therapy or highly active antiretroviral therapy (HAART) for human immunodeficiency virus type 1 (HIV) infection and AIDS has been shown to potently suppress the replication of HIV and extend the life expectancy of HIV-infected individuals (32, 34). Recent analyses have revealed that life expectancy in HIV-infected patients treated with HAART has significantly increased, that mortality rates for HIV-infected persons have recently become close to that of general population, and that the appearance of the current first-line antiretroviral therapy with boosted protease inhibitor (PI)-based regimens has made the development of HIV resistance relatively less likely (2, 7, 18, 39). However, the ability to provide effective long-term antiretroviral therapy for HIV infection remains a complex issue since many of those who initially achieved favorable viral suppression to undetectable levels still suffer treatment failure (12, 18, 29).

Dimerization of HIV protease (PR) subunits is an essential process for the acquisition of proteolytic activity of HIV PR, which plays a critical role in the maturation and replication of the virus (28, 40). Thus, inhibition of PR dimerization by chemical reagents is likely to abolish proteolytic activity and intervene in HIV replication. We have recently developed an intermolecular fluorescence resonance energy transfer (FRET)-based HIV-expression assay that employs cyan fluorescent protein (CFP)- and yellow fluorescent protein (YFP)-tagged HIV PR monomers to detect and quantify PR dimerization (26). Using this assay, we identified a group of nonpeptidyl small molecule inhibitors of HIV PR dimerization. These inhibitors, including darunavir (DRV) and tipranavir (TPV) as well as a series of potent experimental antiretroviral agents such as TMC126 (41), blocked PR dimerization at concentrations of as low as 0.01 μM and potently blocked HIV replication *in vitro* (26).

DRV contains a structure-based and designed privileged nonpeptidic P2 ligand, 3(*R*),3a(*S*),6a(*R*)-*bis*-tetrahydrofuranylurethane (*bis*-THF) (14, 15, 27), which potently inhibits the enzymatic activity and dimerization of HIV PR (26) and has a high-level genetic barrier against HIV development of resistance to DRV (9, 10). Nevertheless, we have witnessed that HIV acquires significant levels of resistance against DRV among HIV-infected individuals who have received long-term combi-

* Corresponding author. Mailing address: Department of Infectious Diseases and Department of Hematology, Kumamoto University School of Medicine, 1-1-1 Honjo, Kumamoto 860-8556, Japan. Phone: (81) 96-373-5156. Fax: (81) 96-363-5265. E-mail: hmitsuya@helix.nih.gov.

▽ Published ahead of print on 3 August 2011.

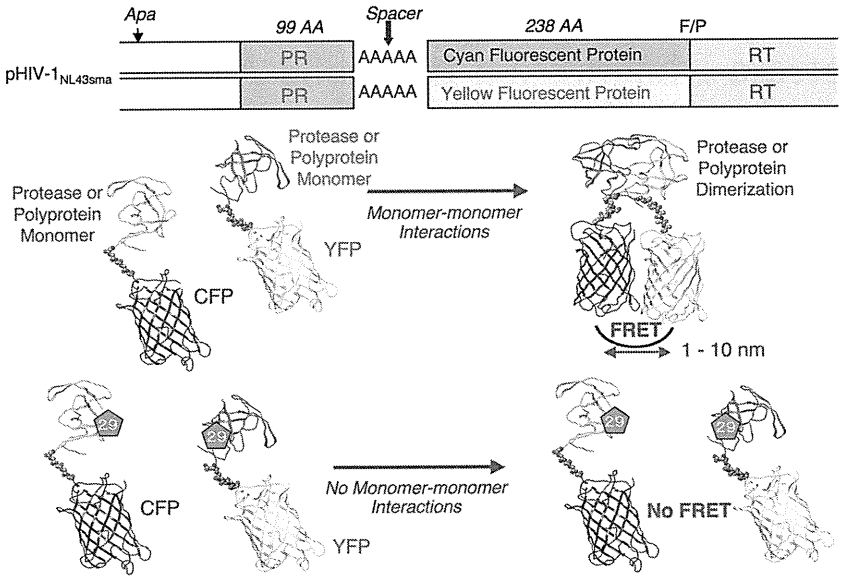

FIG. 1. FRET-based HIV expression system. Plasmids encoding full-length molecular infectious HIV (HIV_{NL4-3}) clones that produce CFP- or YFP-tagged PR were prepared using the PCR-mediated recombination method as described in Materials and Methods. A linker consisting of five alanines was inserted between PR and the fluorescent protein. A phenylalanine-proline site (F/P) that HIV PR cleaves was introduced between the fluorescent protein and RT. Shown are structural representations of PR monomers and dimer in association with the linker atoms and fluorescent proteins. FRET occurs when the two fluorescent proteins become 1 to 10 nm apart. If an agent that is capable of inhibiting the dimerization of PR monomer subunits is present when the CFP- and YFP-tagged PR monomers are produced within the cell upon cotransfection, no FRET occurs. If certain amino acid substitutions (AA) such as D29N (shown below) are introduced, PR subunits do not get dimerized and no FRET occurs.

nation chemotherapy (33, 38). Indeed, a variety of amino acid substitutions that are potentially related to HIV resistance to DRV have been reported (9, 24, 33, 38). Thus, the elucidation of the mechanism of the development of HIV drug resistance represents an urgent subject in the research area of HIV-1 infection/AIDS and therapy.

MATERIALS AND METHODS

Cells, viruses, and antiviral agents. MT-4 cells were grown in RPMI 1640-based culture medium, and 293T and COS7 cells were propagated in Dulbecco's modified Eagle's medium. These media were supplemented with 10% fetal calf serum (FCS; PAA Laboratories GmbH, Linz, Austria) plus 50 U of penicillin and 50 μg of kanamycin per ml. The following HIV strains were used for the determination of 50% effective concentrations (EC_{50}s) against DRV and to construct plasmids for use in the FRET-based HIV expression assay, including HIV_{NL4-3} and $HIV_{8MIX}{}^{P51}$. Three recombinant clinical HIV isolates ($_{rCL}HIV_{F16}$, $_{rCL}HIV_{T45}$, and $_{rCL}HIV_{T48}$) used in this study were produced using recombinant HIV_{NL4-3}-based infectious molecular clones generated by ligating patient-derived amplicons encompassing approximately 200 nucleotides of 3′ Gag (beginning at the unique ApaI restriction site), the entire protease, and the first 72 nucleotides of reverse transcriptase (RT) using the expression vector pNLPFB (a generous gift from Tomozumi Imamichi of the National Institute of Infectious Diseases and Allergy). The four clinical HIV isolates examined in the present study were chosen from 32 isolates that had been obtained from multi-PI-treated patients whose protease genotype contained prototypical patterns of PI resistance. The median duration of continuous PI treatment was 7.5 years (range, 6 to 10 years). The median number of PIs received (excluding the use of ritonavir for pharmacokinetic boosting) was 5 (range, 4 to 8). According to the PhenoSense assay, two isolates ($_{rCL}HIV_{T45}$ and $_{rCL}HIV_{F16}$) had high-level resistance to all PIs, including >90-fold decreased susceptibility to DRV and >8-fold decreased susceptibility to TPV, and one isolate ($_{rCL}HIV_{T48}$) had intermediate resistance to DRV and TPV and high-level resistance to the remaining PIs (see Table 2).

DRV was synthesized by A. K. Ghosh as described previously (16, 27). GRL-0216 (37), GRL-98065 (1), and TMC-126 (41) were synthesized in a convergent manner by coupling an optically active P2 ligand and an (*R*)-hydroxyethylamino sulfonamide isostere (17). TPV was obtained through the AIDS Research and Reference Reagent Program, Division of AIDS, NIAID, National Institutes of Health.

Generation of FRET-based HIV expression system. Cyan fluorescent protein (CFP)- and yellow fluorescent protein (YFP)-tagged HIV PR constructs were generated using BD Creator DNA cloning kits (BD Biosciences, San Jose, CA). The basic concepts of the intermolecular FRET-based HIV expression assay (FRET-HIV assay) are illustrated in Fig. 1. In brief, XhoI and HindIII fragments from the pCR-XL-TOPO vector containing the HIV PR-encoding gene excised from $pHIV_{NL4-3}$ were inserted into pDNR-1r, the donor vector, which had been digested with XhoI and HindIII. In the transfer of the PR gene from the donor vector into pLP-CFP/YFP-C1 (acceptor vector), the Cre-loxP site-specific recombination method was used according to the manufacturer's instructions. Using Cre-recombinase with the loxP site, the PR gene from pDNR-1r was inserted into pLP-CFP-C1 or pLP-YFP-C1 through Cre-mediated recombination (19), generating a plasmid expressing CFP-tagged wild-type PR (PR_{WT}) and one expressing YFP-tagged PR_{WT}, with which HIV PR was successfully expressed as a fusion protein with CFP and YFP tagged at the C terminus, respectively. Western blot assay using anti-green fluorescent protein-specific rabbit polyclonal antibodies revealed that PR was correctly tagged with CFP or YFP (26).

For the generation of full-length molecular infectious clones containing CFP- or YFP-tagged PR, the PCR-mediated recombination (PMR) method was used (11). To this end, we amplified an upstream proviral DNA fragment containing an ApaI site and HIV PR (excised from $pHIV_{NL4-3}$) with primer pair Apa-PRO-F (5′-TTG CAG GGC CCC TAG GAA AAA GG-3′) plus PR-5Ala-R (5′-GGC TGC TGC GGC AGC AAA ATT TAA AGT GCA GCC AAT CT-3′), a middle proviral DNA fragment containing CFP (excised from pCFP-C1) or YFP (excised from pYFP-C1) (Clontech, Mountain View, CA) with primer pair CFPYFP-5Ala-F (5′-GCT GCC GCA GCA GCC GTG AGC AAG GGC GAG GAG CTG-3′) plus CFPYFP-FP-R (5′-ACT AAT GGG AAA CTT GTA CAG CTC GTC CAT GCC G-3′), and a downstream proviral DNA fragment containing the 5′-DNA fragment of RT and an SmaI site from $pHIV_{NLSma}$ (13, 25), which had been created to have an SmaI site by changing two nucleotides (2590 and 2593) of $pHIV_{NL4-3}$, with primer pair FRT-F (5′-TTT CCC ATT AGT CCT ATT GAG ACT GTA-3′) plus NL4-3-RT263-R (5′-CCA GAA ATC TTG AGT TCT CTT ATT-3′). A linker consisting of five alanines was inserted between the PR and fluorescent protein. The phenylalanine-proline site that HIV PR cleaves